Modeling seasonal and vertical habitats of planktonic foraminifera on a global scale

Kerstin Kretschmer[1], Lukas Jonkers[1], Michal Kucera[1], and Michael Schulz[1]

[1]MARUM - Center for Marine Environmental Sciences and Faculty of Geosciences, University of Bremen, Germany.

Correspondence to: Kerstin Kretschmer (kkretschmer@marum.de)

Abstract. Species of planktonic foraminifera exhibit specific seasonal production patterns and different preferred vertical habitats. The seasonality and vertical habitats are not constant throughout the range of the species and changes therein must be considered when interpreting paleoceanographic reconstructions based on fossil foraminifera. Accounting for the effect of vertical and seasonal habitat tracking on foraminifera proxies at times of climate change is difficult because it requires
5 independent fossil evidence. An alternative that could reduce the bias in paleoceanographic reconstructions is to predict species-specific habitat shifts under climate change using an ecosystem modeling approach. To this end, we present a new version of a planktonic foraminifera model, PLAFOM2.0, embedded into the ocean component of the Community Earth System Model, version 1.2.2. This model predicts monthly global concentrations of the planktonic foraminiferal species: *Neogloboquadrina pachyderma*, *N. incompta*, *Globigerina bulloides*, *Globigerinoides ruber* (white), and *Trilobatus sacculifer* throughout the
10 world ocean, resolved in 24 vertical layers to 250 m depth. The resolution along the vertical dimension has been implemented by applying the previously used spatial parameterization of biomass as a function of temperature, light, nutrition, and competition on depth-resolved parameter fields. This approach alone results in the emergence of species-specific vertical habitats, which are spatially and temporally variable. Although an explicit parameterization of the vertical dimension has not been carried out, the seasonal and vertical distribution patterns predicted by the model are in good agreement with sediment trap data and
15 plankton tow observations. In the simulation, the colder-water species *N. pachyderma*, *N. incompta*, and *G. bulloides* show a pronounced seasonal cycle in their depth habitat in the polar and subpolar regions, which appears to be controlled by food availability. During the warm season, these species preferably occur in the subsurface, while towards the cold season they ascend through the water column and are found closer to the sea surface. The warm-water species *G. ruber* (white) and *T. sacculifer* exhibit a less variable shallow depth habitat with highest biomass concentrations within the top 40 m of the water
20 column. Nevertheless, even these species show vertical habitat variability and their seasonal occurrence outside the tropics is limited to the warm surface layer that develops at the end of the warm season. The emergence in PLAFOM2.0 of species-specific vertical habitats that are consistent with observations indicates that the population dynamics of planktonic foraminifera species may be driven by the same factors in time, space, and with depth, in which case the model can provide a reliable and robust tool to aid the interpretation of proxy records.

25 *Copyright statement.*

1 Introduction

Planktonic foraminifera are found throughout the open ocean, where they inhabit roughly the top $500\,\mathrm{m}$ of the water column (Fairbanks et al., 1980, 1982; Kohfeld et al., 1996; Kemle-von Mücke and Oberhänsli, 1999; Mortyn and Charles, 2003; Field, 2004; Kuroyanagi and Kawahata, 2004; Bergami et al., 2009; Wilke et al., 2009; Pados and Spielhagen, 2014; Iwasaki et al.,

5 2017; Rebotim et al., 2017). Their calcareous shells, preserved in ocean sediments, are widely used to reconstruct past climate conditions. To do so, information about their habitat including their horizontal and vertical distribution are needed. It is known from observational data that the prevailing environmental conditions, such as temperature, stratification, light intensity, and food availability, affect the growth and distribution of the individual planktonic foraminifera (Fairbanks et al., 1980, 1982; Bijma et al., 1990b; Watkins et al., 1996; Schiebel et al., 2001; Field, 2004; Kuroyanagi and Kawahata, 2004; Žarić et al.,

10 2005; Salmon et al., 2015; Rebotim et al., 2017).

Based on stratified plankton tow and sediment trap data the seasonal succession of planktonic foraminifera species has been assessed on a local/regional scale (e.g., Fairbanks and Wiebe, 1980; Kohfeld et al., 1996; Wilke et al., 2009; Jonkers et al., 2013; Jonkers and Kučera, 2015), whereas for a broader regional/global perspective modeling approaches have been used to study the seasonal variations in the surface (mixed) layer of the ocean (Žarić et al., 2006; Fraile et al., 2008, 2009a, b;

15 Lombard et al., 2011; Kretschmer et al., 2016). Comparatively less is known about the depth habitat of planktonic foraminifera species and how it varies seasonally. Although previous studies identified different environmental and ontogenetic factors (i.a., temperature, chlorophyll a concentration, the lunar cycle and/or the structure of the water column), which influence the species-specific depth habitats (including their mean living depth and vertical migration) (e.g., Fairbanks and Wiebe, 1980; Fairbanks et al., 1982; Schiebel et al., 2001; Simstich et al., 2003; Field, 2004; Salmon et al., 2015; Rebotim et al., 2017), the only attempt

20 to model the vertical habitat is by Lombard et al. (2011).

It is well known that species-specific habitats vary seasonally and spatially depending on the prevailing climatic conditions (Mix, 1987; Mulitza et al., 1998; Ganssen and Kroon, 2000; Skinner and Elderfield, 2005; Jonkers and Kučera, 2015). Yet, despite this evidence for a variable habitat, it is often assumed in paleoceanographic studies that the habitat of planktonic foraminifera is constant, i.e., it does not change in time and space, potentially leading to erroneous estimates of past climate

25 conditions. Jonkers and Kučera (2017) recently highlighted how foraminifera proxies are affected by habitat tracking and showed that by not accounting for this behavior spatial and temporal trends in proxy records may be underestimated. Given the habitat variability in planktonic foraminifera, it is more than likely that a climate-dependent offset from mean annual sea surface conditions results not only from a seasonal but also from depth habitat variability due to changes in ambient conditions. Such vertical habitat variability was shown by Rebotim et al. (2017) who investigated parameters controlling the depth habitat

30 of planktonic foraminifera in the subtropical eastern North Atlantic. In line with studies from other regions of the world ocean (e.g., Fairbanks et al., 1982; Ortiz et al., 1995; Bijma et al., 1990a; Schiebel et al., 2001; Field, 2004; Salmon et al., 2015), Rebotim et al. (2017) identified distinct species-specific depth habitats, but they also showed that the habitats vary on lunar and seasonal time scales and in response to temperature, chlorophyll a, and other environmental factors. Evidence for variable

depth habitats at least on a regional scale has emerged from studies in other regions (Watkins et al., 1998; Peeters and Brummer, 2002; Kuroyanagi and Kawahata, 2004).

These observations underline the necessity to consider species-specific habitats and their variability on a global scale to increase the reliability of paleoceanographic reconstructions. However, a global assessment of species-specific depth habitat

5 variability in time and space and the potential underlying control mechanisms is lacking. Since the observational data coverage of the global ocean is too sparse to provide in this regard a broad general estimate we apply an ecosystem modeling approach to predict the vertical and seasonal distribution of planktonic foraminifera on a global scale.

2 Methods

2.1 Approach

10 To predict the seasonally varying global species-specific depth habitat of planktonic foraminifera, we modified the previously developed PLAFOM model (Fraile et al., 2008; Kretschmer et al., 2016), which is implemented as an on-line planktonic foraminifera module embedded into the ocean component of the Community Earth System Model, version 1.2.2 (CESM1.2; Hurrell et al., 2013) with the biogeochemical model being enabled (i.e., the CESM1.2(BGC) configuration). This model system simulates the monthly concentrations of five modern planktonic foraminiferal species, which are widely used in paleoceano-

15 graphic reconstructions. The original approach of Fraile et al. (2008) and Kretschmer et al. (2016) aimed for predicting the distribution of planktonic foraminifera in the surface mixed layer at geological time scales. This model version has been successfully used to assess the effect of changing environmental conditions on species distributional patterns in time and space (Fraile et al., 2009a, b; Kretschmer et al., 2016) and to aid in interpreting paleoceanographic records regarding seasonal production shifts in the geological past (Kretschmer et al., 2016), but could not provide any information about depth. To implement

20 the vertical dimension, we used an approach in which we first updated PLAFOM (hereafter referred to as PLAFOM2.0) by including light dependency for symbiont-bearing planktonic foraminifera and then applied the previously used spatial parameterization of biomass as a function of temperature, nutrition, and competition, together with light, on depth-resolved parameter fields. By combining PLAFOM2.0 with the CESM1.2(BGC) configuration the vertical dimension can be resolved throughout the ocean, with 24 layers in the top 250 m.

25 ### 2.2 CESM1.2(BGC) configuration

We used the CESM1.2(BGC) configuration (Moore et al., 2013; Lindsay et al., 2014) as code base. This configuration includes the Biogeochemical Elemental Cycling (BEC) model (Moore et al., 2004, 2006; Krishnamurthy et al., 2007; Moore and Braucher, 2008), which is based on the upper ocean ecosystem model of Moore et al. (2002a, b) coupled to a biogeochemistry model based on the Ocean Carbon Model Intercomparison Project (OCMIP; Doney et al., 2006).

30 The BEC model includes various potentially growth-limiting nutrients (nitrate, ammonium, phosphate, dissolved iron, and silicate), three explicit phytoplankton functional types (diatoms, diazotrophs, pico/nano phytoplankton), a partial calcifier class

(representing coccolithophores), a single adaptive zooplankton class, dissolved organic matter, sinking particulate detritus, and full carbonate system thermodynamics (Moore et al., 2004, 2013). Phytoplankton growth rates are controlled by temperature, light, and available nutrients (Moore et al., 2002b, 2004). The single zooplankton pool grazes on all phytoplankton types, whereby the routing of grazed material varies depending on the type of prey (Moore et al., 2004, 2013). For further details we

5 refer to Moore et al. (2002b, 2004, 2013).

The BEC model has been embedded into the ocean component of CESM, version 1.2.2. CESM1.2 is a fully coupled climate model consisting of several components including the atmosphere, ocean, land, and sea ice (Hurrell et al., 2013), whereby the geophysical fluxes among the components are exchanged through a central coupler (Craig et al., 2012). Here we performed simulations using the ocean model coupled to both the sea ice model and data models for the atmosphere, land, and river

10 routing.

The CESM1.2 ocean component is the Parallel Ocean Program, version 2 (POP2; Smith et al., 2010; Danabasoglu et al., 2012), which is a z-level hydrostatic primitive equation model. Here we use the coarse-resolution configuration of POP2 (Shields et al., 2012), where the longitudinal resolution amounts to $3.6°$ and the latitudinal resolution varies between $1°$ and $2°$, with a finer resolution near the equator. POP2 employs a non-uniform dipolar grid with the North Pole being displaced

15 into Greenland. With a total number of 60 vertical levels, the grid spacing is fine near the surface (10 levels in the top $100\,\mathrm{m}$) and increases with depth to $250\,\mathrm{m}$ near the bottom. The sea ice component of CESM1.2 is the Community Ice Code, version 4 (CICE4; Hunke and Lipscomb, 2008; Holland et al., 2012), which uses the same horizontal grid as the ocean model.

2.3   PLAFOM2.0

This new model version, PLAFOM2.0, considers the polar species *Neogloboquadrina pachyderma*, which is supplemented by

20 the subpolar *N. incompta* (sensu Darling et al., 2006) and *Globigerina bulloides* as well as by the warm-water algal symbiont-bearing species *Globigerinoides ruber* (white) and *Trilobatus sacculifer* (sensu Spezzaferri et al., 2015). Those species have been chosen as they can be considered to represent a large portion of the planktonic foraminiferal biomass in the surface ocean (for further details see Kretschmer et al., 2016). The different planktonic foraminifera species were added as optional passive tracers with the requirement that the BEC model is active.

25 PLAFOM2.0 is driven by temperature, the available food sources (including zooplankton, diatoms, small phytoplankton, and organic detritus), and also light availability, whereby the latter only matters with regard to the growth of the two algal symbiont-bearing species (Erez, 1983; Jørgensen et al., 1985; Gastrich, 1987; Gastrich and Bartha, 1988) and *G. bulloides*, which according to the latest findings hosts the picocyanobacterium *Synechococcus* as a photosynthesizing endobiont (Bird et al., 2017). *Synechococcus* is known to be important for cyanobacterial photosynthesis in marine and freshwater ecosystems

30 (Ting et al., 2002; Jodłowska and Śliwińska, 2014).

The food preferences and temperature tolerance limits for each species have been derived from sediment trap data and culturing experiments (see Fraile et al., 2008, for details). Changes in the foraminifera carbon concentration for each species

are determined as follows:

$$\frac{dF}{dt} = (GGE \cdot TG) - ML \tag{1}$$

where F is the foraminifera carbon concentration (in $\mathrm{mmol\,C\,m^{-3}}$), GGE (gross growth efficiency) is the portion of grazed matter that is incorporated into foraminiferal biomass, TG represents total grazing (i.e., the growth rate in $\mathrm{mmol\,C\,m^{-3}s^{-1}}$),

5   and ML denotes mass loss (i.e., the mortality rate in $\mathrm{mmol\,C\,m^{-3}s^{-1}}$). To properly simulate the vertical distribution of each considered planktonic foraminifera we included light dependency and modified parts of the parameterizations of the foraminiferal species concentration. Therefore, we extended the growth rate equation by not only considering food availability and temperature sensitivity, but also light intensity to define growth. Additionally, we adjusted parts of the mortality rate equation to improve the model accuracy. In the following, the performed modifications are described in detail in regard to the

10   growth and mortality rates. The modifications compared to the earlier model version are summarized in Table 1.

2.3.1   Growth rate

The growth rate depends on the available food and temperature sensitivity of each foraminiferal species as well as on light for the species with algal symbionts and/or cyanobacterial endobionts. To account for the light dependence with depth influencing the growth of *G. bulloides* and of the spinose species *G. ruber* (white) and *T. sacculifer*, we included a photosynthetic growth

15   rate. We applied a similar approach as Doney et al. (1996) and Geider et al. (1998), who determined phytoplankton growth rates by available light and nutrients as used in the BEC model (Moore et al., 2002b, 2004).

Photosynthesis depends on light availability and temperature. This co-dependency can be expressed as follows:

$$P_{F,photo} = P_{F,max} \cdot \left[1 - \exp\left(\frac{-\alpha_{PI} \cdot I_{PAR}}{P_{F,max}} \right) \right]$$

where $P_{F,photo}$ is the foraminiferal specific rate of photosynthesis (in $\mathrm{s^{-1}}$) and $P_{F,max}$ is the maximum value of $P_{F,photo}$ at

20   temperature T (in $\mathrm{s^{-1}}$), calculated as:

$$P_{F,max} = P_{F,0} \cdot T_{func}$$

α_{PI} is the initial slope of the photosynthesis-light curve (in $\mathrm{m^2\,W^{-1}s^{-1}}$) (Table 1), I_{PAR} is the average irradiance over the mixed layer depth provided by the ecosystem model (in $\mathrm{W\,m^{-2}}$), $P_{F,0}$ represents the maximum foraminiferal growth rate at a specific temperature T_0 (in $\mathrm{s^{-1}}$) (Table 1), and T_{func} is the temperature response function (dimensionless). The temperature

25   function is defined as:

$$T_{func} = q_{10}^{\frac{T-T_0}{10}} \tag{2}$$

with a q_{10} value of 1.5 (Sherman et al., 2016) and T being the ambient ocean temperature (in K) and T_0 the reference temperature of $303.15\,\mathrm{K}$.

The photosynthetic growth rate, P_F, in $\mathrm{mmol\,C\,m^{-3}s^{-1}}$, can finally be determined as follows:

30   $$P_F = P_{F,photo} \cdot F \cdot p_\%$$

where $p_\%$ represents the fraction of photosynthesis contributing to growth (see Table 1).

2.3.2 Mortality rate

The mortality rate is determined by respiration loss, predation by higher trophic levels, and competition among species. To improve the seasonal patterns in the foraminiferal biomass for low temperatures we followed Moore et al. (2004) and adjusted the temperature dependence of the predation term (ML_{pred} in $\mathrm{mmol\,C\,m^{-3}s^{-1}}$):

5 $$ML_{pred} = f_{mort2} \cdot T_{func} \cdot F_p^2$$

where f_{mort2} represents the quadratic mortality rate in (in $\mathrm{s^{-1}(mmol\,C\,m^{-3})^{-1}}$), T_{func} is the temperature response function (dimensionless) used for scaling, and F_p (in $\mathrm{mmol\,C\,m^{-3}}$) is used to limit the planktonic foraminifera mortality at very low biomass levels. Compared to Fraile et al. (2008), here predation is scaled by Eq. (2), a temperature function using a q_{10} value of 1.5 (Sherman et al., 2016).

10 Additionally, we included a stronger competitive behavior of *G. bulloides* by adjusting the free parameters in the competition term. In PLAFOM2.0 competition (ML_{comp} in $\mathrm{mmol\,C\,m^{-3}s^{-1}}$) is defined as follows:

$$ML_{comp} = \sum_i \left[F_p \cdot \frac{cl_{ij} \cdot F_i \cdot d}{F_i \cdot d + 0.1} \right]$$

with F_i being the concentration of the foraminiferal species exerting competition, cl_{ij} the maximum competition pressure of species i upon species j, and d the constant controlling the steepness of the Michaelis-Menten relationship for competition. In

15 comparison with Kretschmer et al. (2016), we only modified the parameter cl_{ij} for *N. incompta*, *G. bulloides*, and *G. ruber* (white) (Table 1).

We added the present implementation of PLAFOM2.0 to the code trunk of POP2 as a separate module. Additionally, the food sources for the planktonic foraminifera species are computed in the ecosystem model and instantly passed to PLAFOM2.0 to calculate the foraminifera carbon concentration. For a more detailed description of the planktonic foraminifera model and

20 its behavior on a regional/global scale in the surface mixed layer we refer to Fraile et al. (2008) and Kretschmer et al. (2016).

2.4 Model setup

To test the model we performed a preindustrial-control experiment. Therefore, we derived the initial ocean and sea ice states from an ocean-ice-only simulation, which did not include the BEC ocean biogeochemistry. This model integration was spun-up from rest for 1250 years to approach a quasi steady state by using a climatological forcing (based on atmospheric observations

25 and reanalysis data) as repeated normal year forcing. Heat, freshwater, and momentum fluxes at the sea surface are based on the atmospheric data sets developed by Large and Yeager (2004, 2009) and implemented following the CORE-II-protocol (Coordinated Ocean-ice Reference Experiment) suggested by Griffies et al. (2009).

The tracer fields resulting from the end of this spin-up run were used to initialize the CESM1.2(BGC) preindustrial-control simulation. The biogeochemical tracer fields were, i.a., initialized from data-based climatologies. For instance, initial nutrient

30 (phosphate, nitrate, silicate) distributions were taken from the World Ocean Atlas 2009 (WOA09; Garcia et al., 2010), initial values for dissolved inorganic carbon and alkalinity are from the Global Ocean Data Analysis Project (GLODAP; Key et al.,

2004), whereas zooplankton, phytoplankton pools, and dissolved organic matter have been initialized uniformly at low values (Moore et al., 2004). Additionally, each planktonic foraminiferal species was also initialized uniformly at low values assuming the same (vertical) distribution as the zooplankton component of the BEC model. Furthermore, the atmospheric deposition of iron and dust is based on the climatology of Luo et al. (2003).

5   The CESM1.2(BGC) preindustrial-control simulation was integrated for 200 years to reach stable conditions in the ocean biogeochemistry in the upper $500\,\mathrm{m}$ of the water column (see Figure S1 in the Supplement). Since this simulation has been forced and/or initialized based on climatologies, inter-annual variability and forcing trends can be excluded and therefore we focus our analysis on the model output of only one year, here of year 200.

2.5   Comparison to observations

10   To validate the model performance we compare the simulated spatial and temporal distributions of the considered planktonic foraminiferal species with data from core-tops, sediment traps, and plankton tows (Figure 1). Based on data availability, we focus our analysis on distinct regions distributed over the world ocean covering all climate zones from the poles to the tropics.

2.5.1   Core-top data

To examine the spatial pattern of the five considered planktonic foraminiferal species we compared the model predictions with

15   fossil data by using in total 2844 core-top samples distributed over all oceans (Figure 1a).We combined the Brown University Foraminiferal Database (Prell et al., 1999) with the data assembled by the MARGO project (Kucera et al., 2005), and the data sets provided by Pflaumann et al. (1996, 2003). For the comparison we recalculated the relative abundances of faunal assemblages by only considering those five species used in PLAFOM2.0.

2.5.2   Sediment trap data

20   To compare modeled and observed seasonal production patterns several sediment traps (Table S1 in the Supplement, Figure 1b) have been examined. Those can provide foraminiferal shell fluxes continuously collected over several months or even years. However, some sediment traps comprise only of a few months (i.e., less than a year) and might have just recorded local short-term processes of a particular season/year and can, thus, not provide a long-term/climatological mean.

Here we use the same approach as in Jonkers and Kučera (2015) and present the observed fluxes for multiple years from

25   every location on a $\log_{10}$ scale versus day of year, whereby the zero fluxes have been replaced by half of the observed minimum flux. In this way we can directly compare the peak timings of the measured fluxes at each location with the model, whereby we assume that the flux through the water column (in $\#\,\mathrm{m}^{-2}\,\mathrm{day}^{-1}$) is proportional to the volume integrated model concentrations (in $\mathrm{mmol\,C\,m}^{-3}$).

2.5.3 Plankton tow data

To analyze the vertical distribution, plankton net hauls from different sites distributed across the world ocean (Table S2 in the Supplement, Figure 1b) have been used for a comparison with the simulated vertical distributions. Plankton tow samples have been collected by means of a multiple opening-closing net with a vertical resolution differing between 5 depth levels (one haul)

5   and up to 13 depth levels (two or more consecutive hauls) resolving the upper 100s of meters of the water column. Since the plankton tow data has been collected during a particular time (i.e., a specific day/month) (Table S2), the same month has been considered for the simulated vertical planktonic foraminifera profile for the model-data comparison.

Here we followed the same approach as Rebotim et al. (2017) and calculated an average living depth (ALD) and the vertical dispersion (VD) around the ALD to provide a direct comparison with the modeled depth profile. The ALD (in m) is defined as

10   follows:

$$ALD = \frac{\sum_i C_i \cdot D_i}{\sum_i C_i}$$

with C_i being the foraminiferal species concentration (in $\# \, \mathrm{m}^{-3}$) in the depth interval D_i and VD (in m) is calculated as:

$$VD = \frac{\sum_i (|ALD - D_i| \cdot C_i)}{\sum_i C_i}$$

For further information we refer to Rebotim et al. (2017).

15 ## 3   Results

3.1   Modeled horizontal distribution patterns

The modeled global spatial distribution patterns based on the depth integrated annual mean relative abundances of the five considered foraminiferal species (Figure 2) correspond to the five major provinces of the modern ocean (i.e., polar, subpolar, transitional, subtropical, and tropical) known to be inhabited by those species (Bradshaw, 1959; Bé and Tolderlund, 1971;

20   Hemleben et al., 1989; Kucera, 2007). Note that since the core-top data used for comparison can neither provide any information about the depth habitat of the planktonic foraminiferal species nor about their life cycle the modeled annual mean relative abundances have been obtained by integrating the individual foraminiferal concentrations over the whole water column and by subsequently calculating the percentage of each species relative to the total foraminiferal biomass.

The cold-water species *N. pachyderma* is confined to the high latitudes dominating the polar waters of both hemispheres. *N.*

25   *pachyderma* shows the highest annual mean relative abundances ($> 90\%$) north of the Arctic circle and south of the Antarctic Convergence, whereas toward the subtropics the species' occurrence reduces gradually (Figure 2a). *N. incompta* is mainly found in the subpolar to transitional water masses of the world ocean. This species shows highest annual mean relative abundances ($> 30\%$) in the subantarctic belt as well as in the upwelling region of the equatorial Pacific and in the coastal upwelling systems associated with the cold eastern boundary currents of the Atlantic and Pacific Oceans (Figure 2b). *G. bulloides* exhibits

30   a similar distribution pattern as *N. incompta*. It is present in the subpolar to transitional waters of the world oceans with the

highest annual mean relative abundances ($> 30\%$) occurring in the Southern Ocean, the upwelling areas of the Pacific Ocean, and in the subpolar gyres (Figure 2c). The warm-water species *G. ruber* (white) is mostly confined to the subtropical and tropical regions of both hemispheres whereby the highest annual mean relative abundances of up to 60% are reached in the subtropical gyres (Figure 2d). Lowest annual mean relative abundances can be found in the ocean's upwelling areas especially

5   in the equatorial Pacific cold tongue where *G. ruber* (white) appears to be almost absent. The distribution pattern of *T. sacculifer* is limited to the warm waters of the subtropics and tropics and is similar to the one of *G. ruber* (white). *T. sacculifer* shows highest annual mean relative abundances ($> 50\%$) in the equatorial Pacific between $15\,°N$ and $15\,°S$ and exhibits low annual mean relative abundances ($< 20\%$) in the upwelling regions of the ocean basins (Figure 2e).

3.2   Modeled seasonal distribution

10   For each foraminiferal species the month of maximum production changes on average with temperature and consequently with latitude (Figure 3, Figure S2 in the Supplement). There is a general tendency for the maximum production peak of the cold-water species *N. pachyderma* to occur later in the year (i.e., during summer) for lower annual mean temperatures (Figures 3a and S2a). With increasing mean annual temperatures, however, the peak timing occurs earlier in the year (i.e., during spring) (Figure 3a). For *N. incompta* maximum production is reached during late summer in the midlatitudes at lower temperatures

15   and is shifted towards spring/early summer when temperatures increase (Figure S2b). In the low latitudes at high temperatures, however, peak fluxes of *N. incompta* occur constantly throughout the year (Figure 3b). The peak timing of *G. bulloides* is similar to the peak timing of *N. incompta*, where the highest modeled fluxes are reached later (earlier) in the year in the midlatitudes at lower (higher) temperatures (Figure S2c). In the warm waters (of the tropics) the maximum production of *G. bulloides* occurs year-round (Figure 3c). Both *N. incompta* and *G. bulloides* show indications of a double peak in their timing that is shifted

20   towards the first half of the year when temperatures rise (Figures 3b and 3c). This earlier-when-warmer pattern is also indicated in the peak timing of *N. pachyderma* (Figure 3a). The maximum in the modeled flux of *G. ruber* (white) occurs year-round in the warm waters of the world ocean in the subtropical/tropical regions (Figure S2d). In colder waters (e.g., towards higher latitudes) the maximum production of *G. ruber* (white) is reached in late summer/fall (Figure 3d). A similar seasonal pattern in the peak timing is evident for the tropical species *T. sacculifer* with peak fluxes occurring year-round at high temperatures

25   in the low latitudes (Figure S2e) and in fall when the ambient temperatures are lower (Figure 3e). The peak timing of both *G. ruber* (white) and *T. sacculifer* is shifted to later in the year when the surroundings become colder (Figures 3d and 3e).

Although seasonal changes in the modeled foraminiferal peak fluxes with temperature are evident, all five species exhibit an almost constant peak amplitude (i.e., the maximum concentration divided by the annual mean) in their preferred habitat, which is, i.a., limited by temperature. Outside their preferred living conditions the peak amplitudes increase for most of the species

30   considerably (Figure 3). For the warm-water species *G. ruber* (white) and *T. sacculifer* peak amplitudes rise when the ambient temperatures fall below $20\,°C$ (Figures 3d and 3e). The peak amplitudes of both *N. incompta* and *G. bulloides* increase with temperatures falling below $5\,°C$ (Figures 3b and 3c). Additionally, with temperatures exceeding $25\,°C$ the peak amplitude of *N. incompta* increases (Figure 3b). For the cold-water species *N. pachyderma* the relation between peak amplitudes and mean annual temperatures is more complex (Figure 3a).

3.3 Modeled vertical distribution

Among the three major ocean basins the modeled vertical distribution of each considered planktonic foraminiferal species shows similar patterns in the annual mean (Figure 4). The temperate/cold-water species (i.e., *G. bulloides*, *N. incompta*, and *N. pachyderma*) occur in the surface to subsurface layers up to $200\,\mathrm{m}$ water depth (Figures 4a, 4b and 4c). *N. pachyderma*

5   is consistently present in the top few $100\,\mathrm{m}$ of the water column in the high latitudes and absent in the subtropical/tropical regions. In the polar waters of the three ocean basins maximum annual mean concentrations are found close to the surface and subsequently descend with depth toward lower latitudes. The highest annual mean concentrations of *N. pachyderma* are, however, located in the subpolar gyres between 0 and $80\,\mathrm{m}$ water depth (Figure 4a). *N. incompta* is in general present between $60\,°\mathrm{N}$ and $60\,°\mathrm{S}$ with the annual mean concentration reaching its maximum at around $100\,\mathrm{m}$ water depth. In the mid- to higher

10 latitudes *N. incompta* is found in the surface to subsurface of the Atlantic, Indian, and Pacific Oceans but seems to be largely absent in the respective surface layers of the tropics. However, the annual mean concentration increases with depth especially from the subpolar regions toward the equator (Figure 4b). As for *N. incompta*, *G. bulloides* has been consistently found from the surface to $\sim 200\,\mathrm{m}$ water depth between about $60\,°\mathrm{N}$ and $60\,°\mathrm{S}$. Depending on the ocean basin, maximum annual mean concentrations of *G. bulloides* are either mainly reached at the surface (i.e., in the Indian and Pacific Oceans) or at depth (i.e.,

15 in the Atlantic Ocean), but also subsurface in the subpolar regions of the three chosen transects (Figure 4c).

The warm-water species, *G. ruber* (white) and *T. sacculifer*, are found between the surface of each ocean basin and $100\,\mathrm{m}$ water depth, thus occurring in a shallower depth range compared to *N. pachyderma*, *N. incompta*, and *G. bulloides* (Figures 4d and 4e). Among all five planktonic foraminiferal species, *G. ruber* (white) exhibits the highest annual mean concentrations along the transects (Figure 4). This species is confined to the subtropical/tropical regions of the ocean basins with the highest

20 annual mean concentrations occurring between $20\,°$ and $30\,°$ latitude and the lowest around the equator. Along the transect of the Atlantic Ocean maximum annual mean concentrations are almost consistently reached at depth between 50 and $80\,\mathrm{m}$, whereas in the Indian and Pacific Oceans the annual mean concentrations of *G. ruber* (white) reach their maximum at the surface in the low latitudes and at around $60\,\mathrm{m}$ water depth at those locations where the highest abundance of this species is found (Figure 4d). *T. sacculifer* also occurs predominantly between $30\,°\mathrm{N}$ and $30\,°\mathrm{S}$ with annual mean concentrations gradually decreasing

25 with depth. Compared to the other planktonic foraminiferal species, *T. sacculifer* exhibits a rather uniform distribution pattern along the different transects with the maximum annual mean concentrations being primarily located at the surface (Figure 4e).

3.4 Modeled seasonal variability of habitat depth

In the model the depth of maximum production of each considered planktonic foraminifera changes over the course of a year (Figure 5). Towards higher latitudes *N. incompta* and *N. pachyderma* show in general maximum abundances at lower

30 depth levels compared to low and midlatitudes. In polar regions, *N. pachyderma* occurs close to the surface during winter and descends through the water column from spring to summer with maximum abundances being reached at mid-depth in summer. In the subpolar regions, *N. pachyderma* is generally found at deeper depths between 50 and $100\,\mathrm{m}$ for almost the entire year except for the winter season where highest concentrations are reached close to the surface (Figure 5a). The depth habitat of *N.*

incompta increases from spring to summer and is shallower in winter in the subpolar regions (Figure 5b). In the subtropics and tropics, however, *N. incompta* shows highest concentrations consistently below 90 m depth year-round.

    G. bulloides exhibits a relatively shallow habitat along the equator throughout the year (Figure 5c). In the subpolar regions the depth of maximum production of *G. bulloides* varies seasonally and, similar to *N. incompta*, is shallower during winter and

5 deepest during summer. The depth habitat of *G. ruber* (white) is mostly confined to the top 60 m of the water column and seems to be less variable compared to the temperate and cold-water species (Figure 5). In the midlatitudes highest concentrations of *G. ruber* (white) occur close to the surface during the entire year, whereas in the subtropical/tropical regions this species is most abundant below 20 m and shows a weak seasonal cycle, occurring deeper in late summer/early fall (Figure 5d). *T. sacculifer* exhibits the least variable depth habitat among the five considered species and is consistently found close to the surface above

10 20 m water depth throughout the year (Figure 5e).

4 Discussion

4.1 Large-scale patterns

4.1.1 Geographical range of planktonic foraminifera species

The predicted global distribution patterns of the five considered planktonic foraminiferal species are in good agreement with

15 the core-top data (Figure 2). *N. pachyderma* is most abundant in the polar-subpolar waters of the northern and southern hemispheres both in the model and in the core-top samples (Figure 2a). This cold-water species dominates the waters north of the Arctic circle and south of the Antarctic Convergence with relative abundances exceeding 90% and is very rarely found in subtropical/tropical waters which is also seen in the model output. Bé (1969), Bé and Tolderlund (1971), and Bé and Hutson (1977) showed that *N. pachyderma* mainly occurs in regions with sea surface temperatures (SSTs) below 10 °C but is also

20 present in the cold-temperate waters of, e.g., the subpolar gyres with relative abundances being reduced to 30-50%. Thus, in areas which are influenced by warmer waters the abundance of this species decreases gradually. This is especially evident in the eastern North Atlantic Ocean, where the abundance of *N. pachyderma* is reduced to about 50% due to the influence of the warm Atlantic Water, which is transported northward by the North Atlantic Current (NAC) (Husum and Hald, 2012). In line with the observations, the modeled annual mean relative abundances of *N. pachyderma* also decrease with decreasing latitude and,

25 hence, get reduced towards warmer surface waters (Figure 2a). However, PLAFOM2.0 overestimates this species' abundance in the eastern North Atlantic (i.e., in the area which is influenced by the NAC) compared to the core-top data. This model-data-mismatch might partly arise due to the underlying model parameterizations which are mainly based on the environmental preferences (i.e., temperature tolerance limits) of the *N. pachyderma* genotype found in the Southern Ocean (for more details see Fraile et al., 2008), which differs genetically from the single genotype in the North Atlantic (Darling et al., 2004, 2006).

30 It has been hypothesized that distinct genotypes seem to have different ecological preferences (de Vargas et al., 1999; Darling et al., 2000, 2006; Stewart et al., 2001; Bauch et al., 2003).

The modeled global distribution patterns of *N. incompta* and *G. bulloides* agree in general with the observations (Figures 2b and 2c). Both species predominantly occur in the subarctic/-antarctic and transitional waters of the world oceans (with relative abundances >50%) where the SST ranges between $10°$ and $18°$C (Bé and Tolderlund, 1971; Bé and Hutson, 1977). They are also highly abundant in the cool eastern boundary currents off Africa and South America (e.g., Bé and Tolderlund, 1971;

5 Giraudeau, 1993; Darling et al., 2006) as well as in the eastern North Atlantic and occur continuously in a subantarctic belt between $30°$S and the Antarctic Convergence (Bé, 1969; Bé and Tolderlund, 1971; Boltovskoy et al., 1996). In addition, high abundances (>40%) of *N. incompta* are evident in the equatorial Pacific upwelling system and of *G. bulloides* in the Arabian Sea. The model predictions for both *N. incompta* and *G. bulloides* also show in accordance with the core-top samples higher abundances in the subantarctic belt (here both species account together for up to 90% of the modeled assemblage) and in the

10 (coastal) upwelling regions of the Atlantic and Pacific Oceans. PLAFOM2.0, however, seems to constantly underestimate the relative abundances in those areas where the assemblages are usually dominated by those two species according to the core-top data (Figures 2b and 2c). For instance, in the Benguela upwelling system, *N. incompta* and *G. bulloides* together account locally for >60% of the total planktonic foraminifera population (Bé and Tolderlund, 1971; Giraudeau, 1993) whereas in the model both species only account for $\sim 40\%$ of the assemblage, which is, however, still of the same order of magnitude. Furthermore,

15 in the western Arabian Sea the modeled annual mean relative abundance of *G. bulloides* ranges between 10 and 20% which corresponds to the lower end of the observed range varying between 20 and $\sim 50\%$ (Naidu and Malmgren, 1996). Additionally, it is evident that the model slightly overestimates the species' abundance in the central subtropical/tropical waters of the ocean basins as they are infrequently (<10%) found in the faunal records (Figures 2b and 2c). These apparent discrepancies arise, on the one hand, due to an overestimation of the modeled annual mean abundances of *G. ruber* (white) especially in the

20 upwelling regions. Secondly, since the model parameterizations are performed on a global scale distinct genotypes (possibly having different environmental preferences) of *N. incompta* and especially *G. bulloides* (see, e.g., Kucera and Darling, 2002; Darling and Wade, 2008) cannot be included in detail in the model potentially resulting in the model-data-mismatch.

The simulated global distribution patterns of *G. ruber* (white) and *T. sacculifer* compare favorably with the core-top samples (Figures 2d and 2e). Both species dominate the subtropical and tropical waters of the global ocean together accounting for

25 75-100% of the total planktonic foraminiferal fauna (Bé and Tolderlund, 1971; Bé and Hutson, 1977). *G. ruber* (white) is the most abundant species in the subtropical areas where SSTs range between $21°$ and $29°$C, whereas *T. sacculifer* shows highest relative abundances (>50%) in the tropics with SSTs between $24°$ and $30°$C (Bé and Hutson, 1977). Additionally, *G. ruber* (white) is also highly abundant (>50%) compared to *T. sacculifer* along the continental margins of the low latitudes (Figures 2d and 2e). However, in the coastal upwelling regions *G. ruber* (white) and *T. sacculifer* are rarely found as cooler water masses

30 influence their usual habitat (e.g., Thiede, 1975). Since both species prefer thriving in warmer waters their (relative) abundance gradually diminishes when transported towards the higher latitudes, thus being absent in the subpolar/polar regions of the ocean basins. The model predictions for *G. ruber* (white) and *T. sacculifer* show in general similar patterns as the observations with higher loadings in the subtropical and tropical regions and a gradual decrease in the occurrence toward the poles (Figures 2d and 2e). PLAFOM2.0 is also able to reproduce the dominance of *G. ruber* (white) in the subtropics and of *T. sacculifer* around

35 the equator; and together both species largely account for >70% of the modeled assemblage in the warm waters of the world

ocean. Additionally, the reduction in the (relative) abundances in the upwelling regions (i.e., in the equatorial Pacific and along the coasts of South America and Africa) is likewise captured by the model. However, in those provinces dominated by *G. ruber* (white) and *T. sacculifer* the relative abundances are underestimated in the model, whereas in the coastal upwelling regions the species' abundances are slightly overestimated compared to the observations. Such deviations may result from the over- and/or

5   underestimation of *G. bulloides* and *N. incompta* in the tropical/subtropical or upwelling regions (Figures 2b and 2c) or from the coarse model resolution resulting in a misrepresentation of the coastal upwelling regions.

4.1.2   Seasonality of planktonic foraminifera species

The meta-analysis of Jonkers and Kučera (2015), which is based on sediment trap data, revealed that the (spatially vary-ing) seasonality of individual planktonic foraminifera is predominantly related to either temperature or the timing of primary

10   productivity. For the temperate and cold-water species, such as *G. bulloides*, *N. incompta*, and *N. pachyderma*, one or two flux maxima have been observed, which occur earlier in the year at higher temperatures. This seasonal pattern is also to a large degree evident in the model results (Figures 3a-c and S2a-c). At lower temperatures (below $5\,^{\circ}\text{C}$) the modeled season of maximum production for the cold-water species *N. pachyderma* is predominantly reached in (late) summer, whereas in the comparatively warmer subpolar and transitional waters the modeled peak season is shifted towards spring (Figures 3a and S2a).

15   A similar pattern can be observed for *N. incompta* and *G. bulloides*. In line with Jonkers and Kučera (2015) none of the three species shows a clear dependency of the peak amplitude with temperature (Figure 3a-c). The temperate and cold-water species exhibit a shift in their peak timing but do not considerably change their peak amplitude. Hence, the observed and predicted earlier-when-warmer pattern can most likely be sought in the timing of the primary productivity rather than in a temperature dependence. Several studies showed that the seasonality of the temperate and cold-water planktonic foraminiferal species is

20   closely tied to phytoplankton bloom events leading to an increased food supply (e.g., Fairbanks and Wiebe, 1980; Donner and Wefer, 1994; Wolfteich, 1994; Kohfeld et al., 1996; Mohiuddin et al., 2002, 2004, 2005; Northcote and Neil, 2005; Asahi and Takahashi, 2007; Storz et al., 2009; Wilke et al., 2009; Jonkers and Kučera, 2015). In particular, the flux of *G. bulloides* reaches highest values in response to an increased food supply to a large extent associated with open ocean and/or coastal upwelling (e.g., Thiede, 1975; Curry et al., 1992; Wolfteich, 1994; Naidu and Malmgren, 1996; Kincaid et al., 2000; Mohiuddin et al.,

25   2004, 2005; Storz et al., 2009). The warm-water species *G. ruber* (white) and *T. sacculifer* exhibit relatively uniform annual flux patterns with almost no seasonal peak in the subtropical/tropical regions of the ocean basins (e.g., Deuser et al., 1981; Jonkers and Kučera, 2015). Similar to observations, the modeled timing of the low-amplitude peaks is random during the year in warm waters (Figures 3d-e and S2d-e). However, in colder waters peak fluxes are concentrated towards fall and peak ampli-tudes increase considerably both in the observations and in the model (Figures 3d-e and S2d-e). This shift in the seasonality

30   can most likely be linked to temperature. In the low latitudes optimum temperatures prevail all year round, whereas further north-/southward those optimum thermal conditions occur only during a short period later in the year. Thus, those species focus their flux into the warm season in colder waters (Figure 3d-e). This emerging behavior is consistent with observations from sediment traps (Jonkers and Kučera, 2015) and suggests that the seasonality of the warm-water species is driven by temperature

rather than food availability, which is in agreement with observational studies (e.g., Wolfteich, 1994; Eguchi et al., 1999, 2003; Kincaid et al., 2000; Kuroyanagi et al., 2002; Mohiuddin et al., 2002, 2004; Storz et al., 2009; Jonkers and Kučera, 2015).

4.1.3 Spatial and temporal variability of depth habitats of planktonic foraminifera species

The modeled depth habitats of *N. pachyderma*, *N. incompta*, *G. bulloides*, *G. ruber* (white), and *T. sacculifer* differ among each other and show (distinct) spatial and temporal variability in response to different environmental conditions (Figures 4 and 5). Plankton tow studies have shown that the vertical distribution of planktonic foraminifera is mostly affected by temperature, primary productivity, light availability, and thermal/density stratification of the upper water column (e.g., Fairbanks et al., 1982; Ortiz et al., 1995; Schiebel et al., 2001; Field, 2004; Kuroyanagi and Kawahata, 2004; Salmon et al., 2015; Rebotim et al., 2017).

In line with the observations the modeled depth distribution patterns indicate that the warm-water species *G. ruber* (white) and *T. sacculifer* preferably occur at shallower depths compared to the temperate and cold-water species *G. bulloides*, *N. incompta*, and *N. pachyderma* (see Figures 4 and 5). In the model, both *G. ruber* (white) and *T. sacculifer* have been consistently found from the surface to $\sim 100\,\mathrm{m}$ water depth in the subtropical/tropical regions of the ocean basins (Figure 4d-e). In the tropics they are most abundant close to the surface, which agrees well with the observations. In the Arabian Sea and in the central tropical Pacific Ocean both species have been mostly found in the upper $60\,\mathrm{m}$ (Peeters and Brummer, 2002; Watkins et al., 1996, 1998). In the transitional and subtropical waters, however, PLAFOM2.0 slightly underestimates the depth habitat of *G. ruber* (white) and *T. sacculifer* (Figures 4d-e and 5d-e) as they inhabit the upper $125\,\mathrm{m}$ in the western North Atlantic (Fairbanks et al., 1980) and/or consistently occur from 0 to $200\,\mathrm{m}$ water depth in the subtropical eastern North Atlantic (Rebotim et al., 2017) or in the seas surrounding Japan (Kuroyanagi and Kawahata, 2004). Nevertheless, both species typically live close to the surface (above $100\,\mathrm{m}$) (e.g., Bé and Hamlin, 1967; Fairbanks et al., 1982; Kemle-von Mücke and Oberhänsli, 1999; Schiebel et al., 2002; Wilke et al., 2009; Rippert et al., 2016), thus being associated with a shallow depth habitat, which is reproduced by the model. Since *T. sacculifer* and *G. ruber* (white) are algal symbiont-bearing species they are most abundant in the photic zone where light intensities are highest but also chlorophyll *a* concentrations and temperature control their habitat. Light intensity is especially important for the growth of *T. sacculifer* (Caron et al., 1982, 1987; Jørgensen et al., 1985; Bijma et al., 1990b; Watkins et al., 1998) whereas *G. ruber* (white) seems to be more affected by food availability (Peeters and Brummer, 2002; Field, 2004; Kuroyanagi and Kawahata, 2004; Wilke et al., 2009) rather than light. This would explain why the highest modeled concentrations of *T. sacculifer* occur at shallower depths compared to *G. ruber* (white) (see Figures 4d-e and 5d-e). In comparison with the temperate and cold-water species, *G. ruber* (white) and *T. sacculifer* are most abundant in the model in waters with temperatures above $22\,^{\circ}\mathrm{C}$ and absent where temperature values drop below $15\,^{\circ}\mathrm{C}$ (see Figure 4) reflecting the different temperature tolerance limits of the two species.

N. pachyderma, *N. incompta*, and *G. bulloides* generally thrive in cold to transitional waters. In the model the depth habitat of those species decreases with increasing latitude (Figure 4a-c), indicating a preferred habitat in the subsurface (see Figure 5a-c). This is consistent with the observations from several locations where the three species have typically been found between 50 and $200\,\mathrm{m}$ water depth (e.g., Kohfeld et al., 1996; Mortyn and Charles, 2003; Kuroyanagi and Kawahata, 2004; Bergami

et al., 2009; Wilke et al., 2009; Pados and Spielhagen, 2014; Iwasaki et al., 2017; Rebotim et al., 2017). In the subtropical to subpolar regions the highest modeled concentrations of *G. bulloides* occur, however, between 60 and 100 m, whereas in the tropics maxima are reached close to the surface (Figures 4c and 5c). This agrees well with the observations: *G. bulloides* has been found to be tightly linked to phytoplankton bloom events occurring either at deeper depth layers associated with a

5 deep chlorophyll maximum (DCM) (Fairbanks and Wiebe, 1980; Mortyn and Charles, 2003; Wilke et al., 2009; Iwasaki et al., 2017) or in the coastal and equatorial upwelling regions where a shoaling of the species' habitat towards the near-surface can also be related to high chlorophyll *a* concentrations (Ortiz et al., 1995; Watkins et al., 1998; Peeters and Brummer, 2002; Field, 2004; Kuroyanagi and Kawahata, 2004). *N. incompta* is also highly abundant where chlorophyll *a* concentrations are high, but, nevertheless has most often been observed at mid-depth (Ortiz et al., 1995; Mortyn and Charles, 2003; Field, 2004;

10 Kuroyanagi and Kawahata, 2004; Iwasaki et al., 2017; Rebotim et al., 2017). In the model, *N. incompta* shows also highest concentrations between 30 and 120 m (Figures 4b and 5b), clearly inhabiting the subsurface. This is especially evident in the tropics, where *N. incompta* is absent in the near-surface layers but present, albeit in low numbers, around 100 m water depth. The predictions show, in general, that *N. incompta* prefers warmer waters compared to *N. pachyderma* and where the species co-exist, *N. incompta* inhabits for this reason shallower depths (Figures 4a-b and 5a-b). This agrees with the observations from the

15 subarctic Pacific and the seas around Japan (Iwasaki et al., 2017; Kuroyanagi and Kawahata, 2004). *N. pachyderma* is confined to the high latitudes with peak abundances occurring in the upper 100 m of the water column (Kohfeld et al., 1996; Stangeew, 2001; Mortyn and Charles, 2003; Kuroyanagi and Kawahata, 2004; Bergami et al., 2009; Pados and Spielhagen, 2014) (partly associated with high chlorophyll *a* concentrations), which agrees well with the model results. Although *N. pachyderma* has been classified as a "deep dweller" in different studies (Bé, 1960; Boltovskoy, 1971; Hemleben et al., 1989; Simstich et al.,

20 2003), this species appears to be more surface-restricted at higher latitudes (Carstens and Wefer, 1992; Kohfeld et al., 1996; Mortyn and Charles, 2003), which is also evident in the model results (Figures 4a and 5a).

Several studies showed that the depth habitat of planktonic foraminifera varies throughout a year in response to changing environmental conditions. Rebotim et al. (2017) identified an annual cycle in the habitat of *T. sacculifer* and *N. incompta* in the subtropical eastern North Atlantic. Both species appear to descend in the water column from winter to spring and reach

25 their deepest habitat in spring to summer before ascending again to a shallower depth towards winter (Rebotim et al., 2017). It has been associated that *N. incompta* is affected by chlorophyll *a* concentrations, hence, the seasonal shift in its habitat depth could be related to food availability as a DCM develops in the summer months. In the Canary Islands region *G. ruber* (white) and *G. bulloides* have been found at lower depth levels during winter and during summer/fall shell concentrations where highest at deeper depths associated with the DCM (Wilke et al., 2009). However, *G. ruber* (white) did occur at moderate

30 abundance levels throughout the year, whereas *G. bulloides* was only present in low numbers during wintertime in the study area of Wilke et al. (2009). Peeters and Brummer (2002) investigated the influence of a changing hydrography on the habitat of living planktonic foraminifera in the northwest Arabian Sea. During the southwest monsoon (occurring in summer) strong coastal upwelling associated with low SSTs and a near-surface chlorophyll maximum leads to high abundances of *G. bulloides* dominating the species assemblage in the uppermost part of the water column (Peeters and Brummer, 2002). In comparison,

35 during the northeast monsoon (occurring in winter) a relatively warm nutrient-depleted surface mixed layer as well as a DCM

develop resulting in high concentrations of *G. ruber* (white) and *T. sacculifer* near the surface, whereas the concentrations of *G. bulloides* are low and show a subsurface maximum between the DCM and the thermocline (Peeters and Brummer, 2002). Based on their findings, Peeters and Brummer (2002) conclude that the habitat depth of individual foraminifera strongly depends on the local hydrography controlling, i.a., the food availability. Watkins et al. (1998) also found high abundances of *G.*

5   *bulloides* in the equatorial surface waters of the Pacific Ocean associated with higher primary productivity due to an intensified upwelling but also with the zonal advection by the South Equatorial Current during La Niña conditions. In contrast, during El Niño conditions *G. bulloides* has been absent in the central tropical Pacific (Watkins et al., 1996) due to unfavorable living conditions.

The change in the depth of modeled maximum production of each considered planktonic foraminifera throughout a year

10   (Figure 5) agrees to a large extent with the observations. *N. pachyderma* is almost constantly found in the subsurface (below $50\,\mathrm{m}$) except during winter where highest concentrations occur close to the surface (Figure 5a). The shift in the habitat depth most likely indicates that *N. pachyderma* is highly dependent on food availability (cf. Figure 5a) as this species has been extensively found at mid-depth during summer associated with the chlorophyll maximum (Kohfeld et al., 1996; Mortyn and Charles, 2003; Bergami et al., 2009; Pados and Spielhagen, 2014). The changes from a deeper to shallower depth habitat of *N.*

15   *incompta* in the subpolar regions over the course of a year could be strongly affected by the food supply by potentially following the seasonal distribution of phytoplankton. In the low latitudes maximum concentrations of *N. incompta* are constantly reached in the subsurface, which might be attributed to the presence of a permanent DCM (Figure 5b) being a characteristic feature throughout the low latitudes (Mann and Lazier, 1996). *G. bulloides*, however, is found year-round close to the surface along the equator (Figure 5c), which, in line with the observations, can be associated with equatorial upwelling, but also the inclusion

20   of the photosynthetic growth rate in the model could explain the occurrence of maximum concentration values at lower depth levels due to higher light requirements compared to *N. incompta*. In the subpolar regions the depth habitat of *G. bulloides* varies seasonally most likely following the chlorophyll maximum (Figure 5c). *G. ruber* (white) constantly occurs close to the surface in the midlatitudes due to the prevailing temperature conditions, but in the low latitudes this warm-water species exhibits a weak seasonal cycle in its depth habitat (Figure 5d), indicating its dependence on primary productivity, which agrees with

25   the observations (Peeters and Brummer, 2002; Field, 2004; Kuroyanagi and Kawahata, 2004; Wilke et al., 2009). In line with Kuroyanagi and Kawahata (2004), our results suggest that *T. sacculifer* seems to prefer living in warmer waters than *G. ruber* (white) year-round (Figure 5e) and is most abundant at shallow depths, where the light intensity is highest.

4.2   Comparison with local observations

The emergence of seasonal and vertical habitat patterns consistent with observational data, provides important support for

30   our modeling approach, yet a more detailed comparison with observations is warranted to gain further insight into the model behavior. However, when comparing observational data and model output, one has to bear in mind several caveats. These can be broadly categorized into three groups: i) model resolution, ii) model parameterization, and iii) analytical constraints on the observations.

i) The model resolution has limits on temporal and spatial scales when compared to sediment trap and plankton tow data. Most sediment trap time series span at most a few years and hence represent snapshots that are potentially aliased/biased by inter-annual, seasonal and/or monthly variability, depending on the deployment time. The model, on the other hand, is forced using climatological data, thus representing a long-term average response that ignores such variability. Similarly, plankton tow samples represent even shorter (i.e., daily) snapshots, thus, not being able to reflect a long-term mean, such that the prevailing environmental conditions during their actual sampling time cannot be fully captured by the model. Additionally, because of the rather coarse resolution of the employed model configuration only the nearest model grid points rather than the exact locations of the sediment traps and plankton tows (especially along the coast lines) can be considered. Thus, potentially resulting in different environmental conditions influencing the seasonality and depth habitat of planktonic foraminifera compared to the observations. The observational records are, additionally, affected by sub-grid phenomena (such as mesoscale eddies and/or steep gradients in particular near the coast). For instance, Gulf Stream cold core rings transport large planktonic foraminiferal assemblages into the generally nutrient-poor Sargasso Sea (Fairbanks et al., 1980). In addition, Beckmann et al. (1987) found that an increase in zooplankton (including planktonic foraminifera) productivity coincided with an increase in phytoplankton biomass in a cold-core eddy in the eastern North Atlantic. Due to the coarse resolution of the underlying model configuration such sub-grid processes are not resolved and their impact cannot be reflected by PLAFOM2.0.

ii) The underlying model parameterizations are limited in regard to taxonomic resolution and species' ontogeny. Different morphotypes of one species could exhibit different habitat preferences (e.g., Kuroyanagi and Kawahata, 2004), which is not captured by PLAFOM2.0 since the model parameterizations do not resolve the different known morphotypes of some of the considered planktonic foraminiferal species. Several studies from different areas also showed that the main habitat depth of some species increases from the surface to deeper water layers during shell growth (Peeters and Brummer, 2002; Field, 2004; Iwasaki et al., 2017). This vertical migration of planktonic foraminifera during their ontogeny cannot be reproduced by PLAFOM2.0 as the model parameterizations do not include the individual species' life cycles.

iii) The analytical constraints regarding the observational records include drift due to (sub-grid) ocean processes, distinction between live and dead specimens, collection depths, and taxonomic agreement among different studies. For instance, few sediment trap data might be compromised due to the collection of sinking particles derived from different regions of the surface ocean being transported through eddies and/or ocean currents (Mohiuddin et al., 2004). Strong current velocities sometimes associated with eddies could lead to a tilt in the moored sediment trap resulting in fewer material being collected by the trap (Yu et al., 2001). The impact of eddies might, thus, hamper the observed season of maximum production of planktonic foraminifera as well as their average living depth. A further uncertainty in the plankton tow data arises from the identification of living cells, because dead cells with cytoplasm collected at depth still appear as living and lead to a shift in the average living depth to greater depth (Rebotim et al., 2017). Uneven sampling intervals of the tows also result in a bias in the observed depth habitat (cf. Figure S4). Additionally, a taxonomic consistency within the

observational data is assumed, which cannot be guaranteed as different researchers have been responsible for the data collection (see Tables S1 and S2).

With these caveats in mind, we compare the results of PLAFOM2.0 with 26 sediment trap records and 45 plankton tow samples from all oceans (Figure 1b, Tables S1 and S2). Note that the results of the point-by-point comparative analysis for
5   each site and species are given in the Supplement (see Figures S3 and S4).

The peak season of the temperate and cold-water species is shifted from late summer in the higher latitudes towards spring at the more equatorward directed locations in the subpolar and transitional water masses both in the model and in the sediment trap records (Figure 6a, Table S3a). The modeled peak amplitudes of those species remain almost constant at rather low values independent of the considered region. In the sediment traps, however, the peak amplitude values are higher and more diverse
10   and also no clear pattern is evident neither for the species nor for the provinces changing with latitude (Figure 6b, Table S3b). In line with the plankton tow samples, *N. pachyderma*, *N. incompta*, and *G. bulloides* occur to a large extent in the subsurface from the cold high latitudes to the warmer provinces. However, the modeled ALDs (ranging between 50 and $100\,\mathrm{m}$) are considerably lower than the observed ALDs, which spread over $250\,\mathrm{m}$ (Figure 6c, Table S4). The warm-water species *G. ruber* (white) and *T. sacculifer* occur year-round in the subtropical/tropical regions with no distinct preference for a particular
15   season both in the observations and in the model simulation (Figure 6a, Table S3a). In the transitional waters, however, their peak fluxes are consistently concentrated into fall leading to higher peak amplitude values at least in the model (Figure 6b, Table S3b). Throughout the tropics and subtropics the modeled peak amplitudes remain constant at low values. In the sediment trap records, however, the peak amplitudes are higher (compared with PLAFOM2.0) and vary within both species and within each province (Figure 6b). In the tropics *G. ruber* (white) and *T. sacculifer* occur primarily close to the surface with ALDs
20   below $50\,\mathrm{m}$ both in the model simulation and in the plankton tow records (Figure 6c, Table S4). In fact, the predicted ALD values (consistently ranging between the surface and $55\,\mathrm{m}$) are lower in comparison with the observations in the transitional and subtropical waters and, accordingly, do not exhibit a similar value range as the plankton tow records.

In general, the point-by-point comparison between the observations and the model simulation reveals that the peak seasons are well predicted by PLAFOM2.0. The predicted peak amplitudes and average living depths also show realistic trends, but the
25   model tends to underestimate the magnitude of these trends (cf. Figure 6). Additionally, some sediment trap flux time series of the temperate and cold-water planktonic foraminiferal species show two seasonal peaks a year (cf. Jonkers and Kučera, 2015) (see Figures S3 and 7a). PLAFOM2.0 is, however, not always able to faithfully reproduce this bimodal pattern (cf. Figures S3 and 7a). In the following we try to identify the causes of discrepancies between the observations and predictions by comparing the model output with exemplarily chosen sediment trap records and/or plankton tow samples of three different locations in
30   each case (Figure 7).

The timing of flux pulse(s) of the temperate and cold-water species has, in general, been linked to the timing of the peak in primary productivity (e.g., Fairbanks and Wiebe, 1980; Donner and Wefer, 1994; Wolfteich, 1994; Kohfeld et al., 1996; Mohiuddin et al., 2002, 2004, 2005; Northcote and Neil, 2005; Asahi and Takahashi, 2007; Storz et al., 2009; Wilke et al., 2009; Jonkers and Kučera, 2015). It is known from studies of the North Atlantic Ocean that phytoplankton seasonality changes
35   with latitude, featuring a single spring bloom in the polar and subpolar Atlantic, a bimodal pattern (one large peak in spring, one

smaller peak in fall) in the temperate North Atlantic, a single fall/winter bloom in the subtropical Atlantic, and no prominent seasonal cycle in the tropical Atlantic (e.g., Colebrook, 1979, 1982; Taboada and Anadón, 2014; Friedland et al., 2016). The ecosystem model (providing the food information for PLAFOM2.0), however, does not faithfully reproduce the observed seasonal cycle in the primary productivity (cf. Figure 4 in Moore et al., 2002b). The simulated (depth integrated) chlorophyll

5 concentration, used as an indicator for productivity, does not show two cycles per year (Figure 7a-c). Nevertheless, the peak timings of the (depth integrated) foraminifera concentration follow the maxima in the primary productivity. For instance, the modeled maximum production peak of *N. pachyderma* at site PAPA is preceded by a peak in the diatom concentration (Figure 7a), *N. incompta* reaches its maximum in the simulation more likely at depth at site CP following a DCM (Figure 7b), and *G. bulloides* predicted peak value at site JGOFS34 occurs slightly after the maximum in the chlorophyll concentration (Figure 7c).

10 However, the ecosystem model seems to underestimate the seasonality in the primary productivity, which most likely leads to the model-data-mismatch in the seasonal pattern of the planktonic foraminifera concentration. Additionally, the variability of planktonic foraminifera biomass produced by PLAFOM2.0 is in general too low compared to the observations. This mismatch can either be explained by misrepresentations of the foraminiferal biomass or of the foraminifera response (to the environmental forcing) in the model parameterizations or by an underestimation of the driving factors (i.e., especially the main food sources

15 as outlined above). The depth habitat of planktonic foraminifera depends on several environmental and ontogenetic factors (e.g., Fairbanks and Wiebe, 1980; Fairbanks et al., 1982; Schiebel et al., 2001; Simstich et al., 2003; Field, 2004; Salmon et al., 2015; Rebotim et al., 2017). The simulated vertical distribution patterns can also be related to food availability and temperature (Figure 7d-f). For instance, at station PS78-44 peak abundances of *N. pachyderma* are reached in the top $50\,\mathrm{m}$ in the model corresponding to the highest diatom concentrations (Figure 7d). At station MOC1-28 the predicted depth profile of *G. ruber*

20 (white) coincides with the vertical distribution pattern of zooplankton with both their maxima being reached at $55\,\mathrm{m}$ (Figure 7e). At station SO225-21-3 the modeled species' concentration of *T. sacculifer* decreases gradually with depth following the zooplankton distribution, but also temperature (Figure 7f). However, the simulated depth profiles differ from the observations, which is also indicated by the differences in the ALDs. In PLAFOM2.0 the foraminiferal species do not occur below $200\,\mathrm{m}$ water depth (cf. Figures 4 and 7d-f) most likely being restricted through food availability. Thus, depending on the vertical

25 resolution of the sampling intervals of a plankton tow sample the predicted ALD is very likely lower by several meters than the observed ALD. In summary, PLAFOM2.0 is able to reproduce the observed species' behavior with regard to time and depth on a local scale, but is strongly dependent on the input variables (e.g., the food sources) provided by the ecosystem model and is, thus, limited in its capability to match the observations.

Keeping the caveats regarding the model resolution, model parameterizations, and analytical constraints on the observations

30 in mind, the model-data-mismatch might, however, be reduced by a higher model resolution (in time and space), which would in turn increase the computational costs. A higher taxonomic resolution of the considered species (resulting in an increased number of passive tracers and likewise degrees of freedom) and by explicitly parameterizing the ontogeny of each individual planktonic foraminifera, thus, by considering the changes in the species' life cycles with depth, could considerably improve the model. The discrepancies between the model and the observations could, additionally, be minimized by including better

35 ecological constraints on planktonic foraminifera species and their habitat, e.g., by introducing more phytoplankton and zoo-

plankton functional groups in the ecosystem model to better resolve species' food preferences, which would, however, result in an increased computational cost. Nevertheless, additional knowledge about the factors controlling the habitat of planktonic foraminifera in time and space based on culturing experiments and field studies are needed for an optimization and better validation of the current model version. PLAFOM2.0, however, represents a major step forward from the previous model version

5   and can be used to assess paleoclimate information in a better way.

5   Conclusions

A new version of the dynamic planktonic foraminifera model PLAFOM (PLAFOM2.0), has been developed and combined with the CESM1.2(BGC) model configuration to simulate species-specific seasonal and depth habitats for *N. pachyderma*, *N. incompta*, *G. bulloides*, *G. ruber* (white), and *T. sacculifer* on a global scale. In comparison with the original approach where

10 only species' concentrations in the surface mixed layer were predicted, PLAFOM2.0 includes a vertical component and, thus, predicts species' distribution patterns in space and time more realistically.

PLAFOM2.0 produces spatially and temporally coherent abundance patterns, which agree well with available observations. The model configuration faithfully reproduces the areal extent of the species. In line with core-top data the modeled global distribution of each foraminifera changes with latitude. Additionally, PLAFOM2.0 successfully predicts the patterns in the

15 timing of peak fluxes of planktonic foraminiferal species on a global scale. The earlier-when-warmer pattern for the temperate and cold-water species and the flux focusing at low temperatures of warm-water species, as inferred from observations by Jonkers and Kučera (2015) have emerged from the model.

Although an explicit parameterization of the vertical dimension is lacking, the model successfully predicts the preferred habitat depth of the individual planktonic foraminiferal species as well as the spatial and temporal variability in the vertical

20 abundance. In accordance with the available observations, the warm-water species *G. ruber* (white) and *T. sacculifer* consistently occur close to the sea surface year-round in the tropics/subtropics, whereas the depth habitat of the colder-water species *N. pachyderma*, *N. incompta*, and *G. bulloides* changes seasonally in the polar/subpolar regions. During the cold season these species occur near-surface, while during the warmer season they descend in the water column to be found at mid-depth most likely following the chlorophyll maximum.

25 In general, paleoceanographic reconstructions based on planktonic foraminifera are hampered by the fact that the environmental signal preserved in their shells is the result of both habitat and climate change. The two effects are difficult to separate without independent data. PLAFOM2.0 presents a powerful tool to address this issue and can contribute to more meaningful comparisons of climate model results and paleoclimate reconstructions, ultimately aiding to the understanding of mechanisms of climate change.

30 *Code and data availability.*   All model data can be obtained from the PANGAEA database (www.pangaea.de). The model code is available upon request from the corresponding author (Kerstin Kretschmer, kkretschmer@marum.de).

Competing interests. The authors declare that they have no conflict of interest.

Acknowledgements. We are grateful to Graham Mortyn for providing the plankton tow data from the Atlantic sector of the Southern Ocean.
We would like to thank Gerlinde Jung and Jeroen Groeneveld for their helpful advice. This project was supported by the DFG (Deutsche
Forschungsgemeinschaft) through the International Research Training Group IRTG 1904 ArcTrain.

References

Asahi, H. and Takahashi, K.: A 9-year time-series of planktonic foraminifer fluxes and environmental change in the Bering sea and the central subarctic Pacific Ocean, 1990-1999, Progress in Oceanography, 72, 343–363, https://doi.org/10.1016/j.pocean.2006.03.021, 2007.

Bauch, D., Darling, K., Simstich, J., Bauch, H. A., Erlenkeuser, H., and Kroon, D.: Palaeoceanographic implications of genetic variation in living North Atlantic *Neogloboquadrina pachyderma*, Nature, 424, 299–302, https://doi.org/10.1038/nature01791.1., 2003.

Bé, A. W. H.: Some observations on Arctic planktonic foraminifera, Contrib. Cushman Found. Foram. Res., 11, 64–68, 1960.

Bé, A. W. H.: Planktonic Foraminifera, in: Antarctic Map Folio Series 11: Distribution of Selected Groups of Marine Invertebrates in Waters South of 35ºS Latitude, pp. 9–12, American Geographical Society, 1969.

Bé, A. W. H. and Hamlin, W. H.: Ecology of Recent Planktonic Foraminifera: Part 3: Distribution in the North Atlantic during the Summer of 1962, Micropaleontology, 13, 87–106, 1967.

Bé, A. W. H. and Hutson, W. H.: Ecology of Planktonic Foraminifera and Biogeographic Patterns of Life and Fossil Assemblages in the Indian Ocean, Micropaleontology, 23, 369–414, https://doi.org/10.2307/1485406, 1977.

Bé, A. W. H. and Tolderlund, D. S.: Distribution and ecology of planktonic foraminifera in surface waters of the Atlantic and Indian Oceans, in: The Micropaleontology of Oceans, edited by Funnell, B. and Riedel, W., pp. 105–150, Cambridge University Press, London, 1971.

Beckmann, W., Auras, A., and Hemleben, C.: Cyclonic cold-core eddy in the eastern North Atlantic. III. Zooplankton, Marine Ecology - Progress Series, 39, 165–173, https://doi.org/10.3354/meps039165, 1987.

Bergami, C., Capotondi, L., Langone, L., Giglio, F., and Ravaioli, M.: Distribution of living planktonic foraminifera in the Ross Sea and the Pacific sector of the Southern Ocean (Antarctica), Marine Micropaleontology, 73, 37–48, https://doi.org/10.1016/j.marmicro.2009.06.007, 2009.

Bijma, J., Erez, J., and Hemleben, C.: Lunar and semi-lunar reproductive cycles in some spinose planktonic foraminifers, Journal of Foraminiferal Research, 20, 117–127, 1990a.

Bijma, J., Faber Jr., W. W., and Hemleben, C.: Temperature and salinity limits for growth and survival of some planktonic foraminifers in laboratory cultures, Journal of Foraminiferal Research, 20, 95–116, 1990b.

Bird, C., Darling, K. F., Russell, A. D., Davis, C. V., Fehrenbacher, J., Free, A., Wyman, M., and Ngwenya, B. T.: Cyanobacterial endobionts within a major marine planktonic calcifier (*Globigerina bulloides*, Foraminifera) revealed by 16S rRNA metabarcoding, Biogeosciences, 14, 901–920, https://doi.org/10.5194/bg-14-901-2017, 2017.

Boltovskoy, E.: Planktonic foraminiferal assemblages of the epipelagic zone and their thanatocoenoses, in: The Micropalaeontology of Oceans, edited by Funnell, B. M. and Riedel, W. R., pp. 277–288, Cambridge University Press, London, 1971.

Boltovskoy, E., Boltovskoy, D., Correa, N., and Brandini, F.: Planktic foraminifera from the southwestern Atlantic (30°–60°S): species-specific patterns in the upper 50m, Marine Micropaleontology, 28, 53–72, https://doi.org/10.1016/0377-8398(95)00076-3, 1996.

Bradshaw, J. S.: Ecology of living foraminifera in the North and Equatorial Pacific Ocean, Cushman Foundation for Foraminiferal Research: Contributions, 10, 25–64, 1959.

Caron, D. A., Bé, A. W. H., and Anderson, O. R.: Effects of variations in light intensity on life processes of the planktonic foraminifer *Globigerinoides sacculifer* in laboratory culture, Journal of the Marine Biological Association of the United Kingdom, 62, 435–451, https://doi.org/10.1017/S0025315400057374, 1982.

Caron, D. A., Faber, W. W., and Bé, A. W. H.: Effects of temperature and salinity on the growth and survival of the plank-
tonic foraminifer *Globigerinoides sacculifer*, Journal of the Marine Biological Association of the United Kingdom, 67, 323–341,
https://doi.org/10.1017/S0025315400026643, 1987.

Carstens, J. and Wefer, G.: Recent distribution of planktonic foraminifera in the Nansen Basin, Arctic Ocean, Deep-Sea Research, 39, S507–
S524, 1992.

Colebrook, J. M.: Continuous Plankton Records: Seasonal Cycles of Phytoplankton and Copepods in the North Atlantic Ocean and the North
Sea, Marine Biology, 51, 23–32, https://doi.org/10.1016/0011-7471(66)90628-0, 1979.

Colebrook, J. M.: Continuous plankton records: seasonal variations in the distribution and abundance of plankton in the North Atlantic Ocean
and the North Sea, Journal of Plankton Research, 4, 435–462, 1982.

Craig, A. P., Vertenstein, M., and Jacob, R.: A New Flexible Coupler for Earth System Modeling developed for CCSM4 and CESM1,
International Journal of High Performance Computing Applications, 26, 31–42, https://doi.org/10.1177/1094342011428141, 2012.

Curry, W. B., Ostermann, D. R., Guptha, M. V. S., and Ittekkot, V.: Foraminiferal production and monsoonal up-
welling in the Arabian Sea: evidence from sediment traps, Geological Society, London, Special Publications, 64, 93–106,
https://doi.org/10.1144/GSL.SP.1992.064.01.06, 1992.

Danabasoglu, G., Bates, S. C., Briegleb, B. P., Jayne, S. R., Jochum, M., Large, W. G., Peacock, S., and Yeager, S. G.: The CCSM4 Ocean
Component, Journal of Climate, 25, 1361–1389, https://doi.org/10.1175/JCLI-D-11-00091.1, 2012.

Darling, K. F. and Wade, C. M.: The genetic diversity of planktic foraminifera and the global distribution of ribosomal RNA genotypes,
Marine Micropaleontology, 67, 216–238, https://doi.org/10.1016/j.marmicro.2008.01.009, 2008.

Darling, K. F., Wade, C. M., Stewart, I. A., Kroon, D., Dingle, R., and Brown, A. J. L.: Molecular evidence for genetic mixing of Arctic and
Antarctic subpolar populations of planktonic foraminifers, Nature, 405, 43–47, https://doi.org/10.1038/35011002, 2000.

Darling, K. F., Kucera, M., Pudsey, C. J., and Wade, C. M.: Molecular evidence links cryptic diversification in polar planktonic protists to
Quaternary climate dynamics, PNAS, 101, 7657–7662, 2004.

Darling, K. F., Kucera, M., Kroon, D., and Wade, C. M.: A resolution for the coiling direction paradox in *Neogloboquadrina pachyderma*,
Paleoceanography, 21, PA2011, https://doi.org/10.1029/2005PA001189, 2006.

de Vargas, C., Norris, R., Zaninetti, L., Gibb, S. W., and Pawlowski, J.: Molecular evidence of cryptic speciation in planktonic foraminifers
and their relation to oceanic provinces., Proc. Natl. Acad. Sci., USA, 96, 2864–2868, https://doi.org/10.1073/pnas.96.6.2864, 1999.

Deuser, W. G., Ross, E. H., Hemleben, C., and Spindler, M.: Seasonal changes in species composition, numbers, mass, size, and isotopic
composition of planktonic foraminifera settling into the deep Sargasso Sea, Palaeogeography, Palaeoclimatology, Palaeoecology, 33, 103–
127, https://doi.org/10.1016/0031-0182(81)90034-1, 1981.

Doney, S. C., Glover, D. M., and Najjar, R. G.: A new coupled, one-dimensional biological-physical model for the upper ocean: Applications
to the JGOFS Bermuda Atlantic Time-series Study (BATS) site, Deep Sea Research Part II: Topical Studies in Oceanography, 43, 591–624,
https://doi.org/10.1016/0967-0645(95)00104-2, 1996.

Doney, S. C., Lindsay, K., Fung, I., and John, J.: Natural Variability in a Stable, 1000-Yr Global Coupled Climate-Carbon Cycle Simulation,
Journal of Climate, 19, 3033–3054, https://doi.org/10.1175/JCLI3783.1, 2006.

Donner, B. and Wefer, G.: Flux and stable isotope composition of *Neogloboquadrina pachyderma* and other planktonic foraminifers in the
Southern Ocean (Atlantic sector), Deep-Sea Research I, 41, 1733–1743, 1994.

Eguchi, N. O., Kawahata, H., and Taira, A.: Seasonal Response of Planktonic Foraminifera to Surface Ocean Condition: Sediment Trap
Results from the Central North Pacific Ocean, Journal of Oceanography, 55, 681–691, 1999.

Eguchi, N. O., Ujiié, H., Kawahata, H., and Taira, A.: Seasonal variations in planktonic foraminifera at three sediment traps in the Subarctic, Transition and Subtropical zones of the central North Pacific Ocean, Marine Micropaleontology, 48, 149–163, https://doi.org/10.1016/S0377-8398(03)00020-3, 2003.

Erez, J.: Calcification Rates, Photosynthesis and Light in Planktonic Foraminifera, in: Biomineralization and Biological Metal Accumulation: Biological and Geological Perspectives Papers presented at the Fourth International Symposium on Biomineralization, Renesse, The Netherlands, June 2–5, 1982, edited by Westbroek, P. and de Jong, E. W., pp. 307–312, Springer Netherlands, Dordrecht, The Netherlands, https://doi.org/10.1007/978-94-009-7944-4_29, 1983.

Fairbanks, R. G. and Wiebe, P. H.: Foraminifera and Chlorophyll Maximum: Vertical Distribution, Seasonal Succession, and Paleoceanographic Significance, Science, 209, 1524–1526, 1980.

Fairbanks, R. G., Wiebe, P. H., and Bé, A. W. H.: Vertical Distribution and Isotopic Composition of Living Planktonic Foraminifera in the Western North Atlantic, Science, 207, 61–63, 1980.

Fairbanks, R. G., Sverdlove, M., Free, R., Wiebe, P. H., and Bé, A. W. H.: Vertical distribution and isotopic fractionation of living planktonic foraminifera from the Panama Basin, Nature, 298, 841–844, 1982.

Field, D. B.: Variability in vertical distributions of planktonic foraminifera in the California Current: Relationships to vertical ocean structure, Paleoceanography, 19, PA2014, https://doi.org/10.1029/2003PA000970, 2004.

Fraile, I., Schulz, M., Mulitza, S., and Kucera, M.: Predicting the global distribution of planktonic foraminifera using a dynamic ecosystem model, Biogeosciences, 5, 891–911, 2008.

Fraile, I., Mulitza, S., and Schulz, M.: Modeling planktonic foraminiferal seasonality: Implications for sea-surface temperature reconstructions, Marine Micropaleontology, 72, 1–9, https://doi.org/10.1016/j.marmicro.2009.01.003, 2009a.

Fraile, I., Schulz, M., Mulitza, S., Merkel, U., Prange, M., and Paul, A.: Modeling the seasonal distribution of planktonic foraminifera during the Last Glacial Maximum, Paleoceanography, 24, PA2216, https://doi.org/10.1029/2008PA001686, 2009b.

Friedland, K. D., Record, N. R., Asch, R. G., Kristiansen, T., Saba, V. S., Drinkwater, K. F., Henson, S., Leaf, R. T., Morse, R. E., Johns, D. G., Large, S. I., Hjøllo, S. S., Nye, J. A., Alexander, M. A., and Ji, R.: Seasonal phytoplankton blooms in the North Atlantic linked to the overwintering strategies of copepods, Elementa: Science of the Anthropocene, 4, 000099, https://doi.org/10.12952/journal.elementa.000099, 2016.

Ganssen, G. M. and Kroon, D.: The isotopic signature of planktonic foraminifera from NE Atlantic surface sediments: implications for the reconstruction of past oceanic conditions, Journal of the Geological Society, London, 157, 693–699, https://doi.org/10.1144/jgs.157.3.693, 2000.

Garcia, H. E., Locarnini, R. A., Boyer, T. P., Antonov, J. I., Zweng, M. M., Baranova, O. K., and Johnson, D. R.: World Ocean Atlas 2009, Volume 4: Nutrients (phosphate, nitrate, silicate)., U.S. Government Printing Office, Washington, D.C., https://doi.org/10.1182/blood-2011-06-357442, 2010.

Gastrich, M. D.: Ultrastructure of a new intracellular symbiotic alga found within planktonic foraminifera, Journal of Phycology, 23, 623–632, https://doi.org/10.1111/j.1529-8817.1987.tb04215.x, 1987.

Gastrich, M. D. and Bartha, R.: Primary productivity in the planktonic foraminifer *Globigerinoides ruber* (D'Orbigny), Journal of Foraminiferal Research, 18, 137–142, 1988.

Geider, R. J., MacIntyre, H. L., and Kana, T. M.: A dynamic regulatory model of phytoplanktonic acclimation to light, nutrients, and temperature, Limnol. Oceanography, 43, 679–694, 1998.

Giraudeau, J.: Planktonic foraminiferal assemblages in surface sediments from the south western African continental margin, Marine Geology, 110, 47–62, https://doi.org/10.1016/0025-3227(93)90104-4, 1993.

Griffies, S. M., Biastoch, A., Böning, C., Bryan, F., Danabasoglu, G., Chassignet, E. P., England, M. H., Gerdes, R., Haak, H., Hallberg, R. W., Hazeleger, W., Jungclaus, J., Large, W. G., Madec, G., Pirani, A., Samuels, B. L., Scheinert, M., Gupta, A. S., Severijns, C. A., Simmons, H. L., Treguier, A. M., Winton, M., Yeager, S., and Yin, J.: Coordinated Ocean-ice Reference Experiments (COREs), Ocean Modelling, 26, 1–46, https://doi.org/10.1016/j.ocemod.2008.08.007, 2009.

Hemleben, C., Spindler, M., and Anderson, O. R.: Modern Planktonic Foraminifera, Springer, New York, 1989.

Holland, M. M., Bailey, D. A., Briegleb, B. P., Light, B., and Hunke, E.: Improved Sea Ice Shortwave Radiation Physics in CCSM4: The Impact of Melt Ponds and Aerosols on Arctic Sea Ice, Journal of Climate, 25, 1413–1430, https://doi.org/10.1175/JCLI-D-11-00078.1, 2012.

Hunke, E. C. and Lipscomb, W. H.: CICE: The Los Alamos Sea Ice Model, Documentation and Software User's Manual, Version 4.0, Tech. rep., Los Alamos National Laboratory, 2008.

Hurrell, J. W., Holland, M. M., Gent, P. R., Ghan, S., Kay, J. E., Kushner, P. J., Lamarque, J.-F., Large, W. G., Lawrence, D., Lindsay, K., Lipscomb, W. H., Long, M. C., Mahowald, N., Marsh, D. R., Neale, R. B., Rasch, P., Vavrus, S., Vertenstein, M., Bader, D., Collins, W. D., Hack, J. J., Kiehl, J., and Marshall, S.: The Community Earth System Model: A framework for collaborative research, Bulletin of the American Meteorological Society, 94, 1339–1360, https://doi.org/10.1175/BAMS-D-12-00121.1, 2013.

Husum, K. and Hald, M.: Arctic planktic foraminiferal assemblages: Implications for subsurface temperature reconstructions, Marine Micropaleontology, 96-97, 38–47, https://doi.org/10.1016/j.marmicro.2012.07.001, 2012.

Iwasaki, S., Kimoto, K., Kuroyanagi, A., and Kawahata, H.: Horizontal and vertical distributions of planktic foraminifera in the subarctic Pacific, Marine Micropaleontology, 130, 1–14, https://doi.org/10.1016/j.marmicro.2016.12.001, 2017.

Jodłowska, S. and Śliwińska, S.: Effects of light intensity and temperature on the photosynthetic irradiance response curves and chlorophyll fluorescence in three picocyanobacterial strains of *Synechococcus*, Photosynthetica, 52, 223–232, https://doi.org/10.1007/s11099-014-0024-y, 2014.

Jonkers, L. and Kučera, M.: Global analysis of seasonality in the shell flux of extant planktonic Foraminifera, Biogeosciences, 12, 2207–2226, https://doi.org/10.5194/bg-12-2207-2015, 2015.

Jonkers, L. and Kučera, M.: Quantifying the effect of seasonal and vertical habitat tracking on planktonic foraminifera proxies, Climate of the Past, 13, 573–586, https://doi.org/10.5194/cp-13-573-2017, 2017.

Jonkers, L., van Heuven, S., Zahn, R., and Peeters, F. J. C.: Seasonal patterns of shell flux, δ^{18}O and δ^{13}C of small and large *N. pachyderma* (s) and *G. bulloides* in the subpolar North Atlantic, Paleoceanography, 28, 164–174, https://doi.org/10.1002/palo.20018, 2013.

Jørgensen, B. B., Erez, J., Revsbech, N. P., and Cohen, Y.: Symbiotic photosynthesis in a planktonic foraminiferan, *Globigerinoides sacculifer* (Brady), studied with microelectrodes, Limnology and Oceanography, 30, 1253–1267, https://doi.org/10.4319/lo.1985.30.6.1253, 1985.

Kemle-von Mücke, S. and Oberhänsli, H.: The Distribution of Living Planktic Foraminifera in Relation to Southeast Atlantic Oceanography, in: Use of Proxies in Paleoceanography, pp. 91–115, Springer, Berlin, Heidelberg, 1999.

Key, R. M., Kozyr, A., Sabine, C. L., Lee, K., Wanninkhof, R., Bullister, J. L., Feely, R. A., Millero, F. J., Mordy, C., and Peng, T.-H.: A global ocean carbon climatology: Results from Global Data Analysis Project (GLODAP), Global Biogeochemical Cycles, 18, GB4031, https://doi.org/10.1029/2004GB002247, 2004.

Kincaid, E., Thunell, R. C., Le, J., Lange, C. B., Weinheimer, A. L., and Reid, F. M. H.: Planktonic foraminiferal fluxes in the Santa Barbara Basin: response to seasonal and interannual hydrographic changes, Deep-Sea Research Part II, 47, 1157–1176, https://doi.org/10.1016/S0967-0645(99)00140-X, 2000.

Kohfeld, K. E., Fairbanks, R. G., Smith, S. L., and Walsh, I. D.: *Neogloboquadrina pachyderma* (sinistral coiling) as paleoceanographic tracers in polar oceans: Evidence from Northeast Water Polynya plankton tows, sediment traps, and surface sediments, Paleoceanography, 11, 679–699, 1996.

Kretschmer, K., Kucera, M., and Schulz, M.: Modeling the distribution and seasonality of *Neogloboquadrina pachyderma* in the North Atlantic Ocean during Heinrich Stadial 1, Paleoceanography, 31, 1–25, https://doi.org/10.1002/2015PA002819, 2016.

Krishnamurthy, A., Moore, J. K., Zender, C. S., and Luo, C.: Effects of atmospheric inorganic nitrogen deposition on ocean biogeochemistry, Journal of Geophysical Research, 112, G02019, https://doi.org/10.1029/2006JG000334, 2007.

Kucera, M.: Planktonic Foraminifera as Tracers of Past Oceanic Environments, in: Proxies in Late Cenozoic Paleoceanography, edited by Hillaire-Marcel, C. and de Vernal, A., chap. 6, pp. 213–262, Elsevier, Amsterdam, https://doi.org/10.1016/S1572-5480(07)01011-1, 2007.

Kucera, M. and Darling, K. F.: Cryptic species of planktonic foraminifera: their effect on palaeoceanographic reconstructions, Philosophical Transactions of the Royal Society of London Series A, 360, 695–718, 2002.

Kucera, M., Weinelt, M., Kiefer, T., Pflaumann, U., Hayes, A., Weinelt, M., Chen, M.-T., Mix, A. C., Barrows, T. T., Cortijo, E., Duprat, J., Juggins, S., and Waelbroeck, C.: Reconstruction of sea-surface temperatures from assemblages of planktonic foraminifera: multi-technique approach based on geographically constrained calibration data sets and its application to glacial Atlantic and Pacific Oceans, Quaternary Science Reviews, 24, 951–998, https://doi.org/10.1016/j.quascirev.2004.07.014, 2005.

Kuroyanagi, A. and Kawahata, H.: Vertical distribution of living planktonic foraminifera in the seas around Japan, Marine Micropaleontology, 53, 173–196, https://doi.org/10.1016/j.marmicro.2004.06.001, 2004.

Kuroyanagi, A., Kawahata, H., Nishi, H., and Honda, M. C.: Seasonal changes in planktonic foraminifera in the northwestern North Pacific Ocean: sediment trap experiments from subarctic and subtropical gyres, Deep-Sea Research Part II, 49, 5627–5645, https://doi.org/10.1016/S0967-0645(02)00202-3, 2002.

Large, W. G. and Yeager, S. G.: Diurnal to Decadal Global Forcing For Ocean and Sea-Ice Models: The Data Sets and Flux Climatologies, Tech. Rep. May, NCAR Technical Note NCAR/TN-460+STR, 2004.

Large, W. G. and Yeager, S. G.: The global climatology of an interannually varying air–sea flux data set, Climate Dynamics, 33, 341–364, https://doi.org/10.1007/s00382-008-0441-3, 2009.

Lindsay, K., Bonan, G. B., Doney, S. C., Hoffman, F. M., Lawrence, D. M., Long, M. C., Mahowald, N. M., Moore, J. K., Randerson, J. T., and Thornton, P. E.: Preindustrial-Control and Twentieth-Century Carbon Cycle Experiments with the Earth System Model CESM1(BGC), Journal of Climate, 27, 8981–9005, https://doi.org/10.1175/JCLI-D-12-00565.1, 2014.

Lombard, F., Labeyrie, L., Michel, E., Bopp, L., Cortijo, E., Retailleau, S., Howa, H., and Jorissen, F.: Modelling planktic foraminifer growth and distribution using an ecophysiological multi-species approach, Biogeosciences, 8, 853–873, https://doi.org/10.5194/bg-8-853-2011, 2011.

Luo, C., Mahowald, N. M., and del Corral, J.: Sensitivity study of meteorological parameters on mineral aerosol mobilization, transport, and distribution, Journal of Geophysical Research, 108, 4447, https://doi.org/10.1029/2003JD003483, 2003.

Mann, K. H. and Lazier, J. R. N.: Dynamics of Marine Ecosystems: Biological-Physical Interactions in the Oceans, Blackwell Publishing Ltd, 2nd edn., 1996.

Mix, A. C.: The oxygen-isotope record of glaciation, in: The Geology of North America, chap. 6, pp. 111–135, The Geological Society of America, 1987.

Mohiuddin, M. M., Nishimura, A., Tanaka, Y., and Shimamoto, A.: Regional and interannual productivity of biogenic components and planktonic foraminiferal fluxes in the northwestern Pacific Basin, Marine Micropaleontology, 45, 57–82, https://doi.org/10.1016/S0377-8398(01)00045-7, 2002.

Mohiuddin, M. M., Nishimura, A., Tanaka, Y., and Shimamoto, A.: Seasonality of biogenic particle and planktonic foraminifera fluxes: Response to hydrographic variability in the Kuroshio Extension, northwestern Pacific Ocean, Deep-Sea Research Part I, 51, 1659–1683, https://doi.org/10.1016/j.dsr.2004.06.002, 2004.

Mohiuddin, M. M., Nishimura, A., and Tanaka, Y.: Seasonal succession, vertical distribution, and dissolution of planktonic foraminifera along the Subarctic Front: Implications for paleoceanographic reconstruction in the northwestern Pacific, Marine Micropaleontology, 55, 129–156, https://doi.org/10.1016/j.marmicro.2005.02.007, 2005.

Moore, J. K. and Braucher, O.: Sedimentary and mineral dust sources of dissolved iron to the world ocean, Biogeosciences, 5, 631–656, 2008.

Moore, J. K., Doney, S. C., Glover, D. M., and Fung, I. Y.: Iron cycling and nutrient-limitation patterns in surface waters of the World Ocean, Deep Sea Research II, 49, 463–507, 2002a.

Moore, J. K., Doney, S. C., Kleypas, J. A., Glover, D. M., and Fung, I. Y.: An intermediate complexity marine ecosystem model for the global domain, Deep Sea Research II, 49, 403–462, 2002b.

Moore, J. K., Doney, S. C., and Lindsay, K.: Upper ocean ecosystem dynamics and iron cycling in a global three-dimensional model, Global Biogeochemical Cycles, 18, GB4028, https://doi.org/10.1029/2004GB002220, 2004.

Moore, J. K., Doney, S. C., Lindsay, K., Mahowald, N., and Michaels, A. F.: Nitrogen fixation amplifies the ocean biogeochemical response to decadal timescale variations in mineral dust deposition, Tellus, 58B, 560–572, https://doi.org/10.1111/j.1600-0889.2006.00209.x, 2006.

Moore, J. K., Lindsay, K., Doney, S. C., Long, M. C., and Misumi, K.: Marine Ecosystem Dynamics and Biogeochemical Cycling in the Community Earth System Model [CESM1(BGC)]: Comparison of the 1990s with the 2090s under the RCP4.5 and RCP8.5 Scenarios, Journal of Climate, 26, 9291–9312, https://doi.org/10.1175/JCLI-D-12-00566.1, 2013.

Mortyn, P. G. and Charles, C. D.: Planktonic foraminiferal depth habitat and δ^{18}O calibrations: Plankton tow results from the Atlantic sector of the Southern Ocean, Paleoceanography, 18, 1037, https://doi.org/10.1029/2001PA000637, 2003.

Mulitza, S., Wolff, T., Pätzold, J., Hale, W., and Wefer, G.: Temperature sensitivity of planktic foraminifera and its influence on the oxygen isotope record, Marine Micropaleontology, 33, 223–240, 1998.

Naidu, P. D. and Malmgren, B. A.: A high-resolution record of late Quaternary upwelling along the Oman Margin, Arabian Sea based on planktonic foraminifera, Paleoceanography, 11, 129–140, 1996.

Northcote, L. C. and Neil, H. L.: Seasonal variations in foraminiferal flux in the Southern Ocean, Campbell Plateau, New Zealand, Marine Micropaleontology, 56, 122–137, https://doi.org/10.1016/j.marmicro.2005.05.001, 2005.

Ortiz, J. D., Mix, A. C., and Collier, R. W.: Environmental control of living symbiotic and asymbiotic foraminifera of the California Current, Paleoceanography, 10, 987–1009, 1995.

Pados, T. and Spielhagen, R. F.: Species distribution and depth habitat of recent planktic foraminifera in Fram Strait, Arctic Ocean, Polar Research, 33, 22483, https://doi.org/10.3402/polar.v33.22483, 2014.

Peeters, F. J. C. and Brummer, G.-J. A.: The seasonal and vertical distribution of living planktic foraminifera in the NW Arabian Sea, Geological Society, London, Special Publications, 195, 463–497, https://doi.org/10.1144/GSL.SP.2002.195.01.26, 2002.

Pflaumann, U., Duprat, J., Pujol, C., and Labeyrie, L. D.: SIMMAX: A modern analog technique to deduce Atlantic sea surface temperatures from planktonic foraminifera in deep-sea sediments, Paleoceanography, 11, 15–35, 1996.

Pflaumann, U., Sarnthein, M., Chapman, M., de Abreu, L., Funnell, B., Huels, M., Kiefer, T., Maslin, M., Schulz, H., Swallow, J., van Kreveld, S., Vautravers, M., Vogelsang, E., and Weinelt, M.: Glacial North Atlantic: Sea-surface conditions reconstructed by GLAMAP 2000, Paleoceanography, 18, 1065, https://doi.org/10.1029/2002PA000774, 2003.

Prell, W. L., Martin, A., Cullen, J. L., and Trend, M.: The Brown University Foraminiferal Data Base, IGBP PAGES/World Data Center-A for Paleoclimatology, Data Contribution Series # 1999-027, NOAA/NGDC Paleoclimatology Program, Boulder CO, USA, https://www.ncdc.noaa.gov/paleo/metadata/noaa-ocean-5908.html, 1999.

Rebotim, A., Voelker, A. H. L., Jonkers, L., Waniek, J. J., Meggers, H., Schiebel, R., Fraile, I., Schulz, M., and Kucera, M.: Factors controlling the depth habitat of planktonic foraminifera in the subtropical eastern North Atlantic, Biogeosciences, 14, 827–859, https://doi.org/10.5194/bg-14-827-2017, 2017.

Rippert, N., Nürnberg, D., Raddatz, J., Maier, E., Hathorne, E., Bijma, J., and Tiedemann, R.: Constraining foraminiferal calcification depths in the western Pacific warm pool, Marine Micropaleontology, 128, 14–27, https://doi.org/10.1016/j.marmicro.2016.08.004, 2016.

Salmon, K. H., Anand, P., Sexton, P. F., and Conte, M.: Upper ocean mixing controls the seasonality of planktonic foraminifer fluxes and associated strength of the carbonate pump in the oligotrophic North Atlantic, Biogeosciences, 12, 223–235, https://doi.org/10.5194/bg-12-223-2015, 2015.

Schiebel, R., Waniek, J., Bork, M., and Hemleben, C.: Planktic foraminiferal production stimulated by chlorophyll redistribution and entrainment of nutrients, Deep-Sea Research Part I: Oceanographic Research Papers, 48, 721–740, 2001.

Schiebel, R., Waniek, J., Zeltner, A., and Alves, M.: Impact of the Azores Front on the distribution of planktic foraminifers, shelled gastropods, and coccolithophorids, Deep-Sea Research Part II, 49, 4035–4050, 2002.

Sherman, E., Moore, J. K., Primeau, F., and Tanouye, D.: Temperature influence on phytoplankton community growth rates, Global Biogeochem. Cycles, 30, 550–559, https://doi.org/10.1002/2015GB005272.Received, 2016.

Shields, C. A., Bailey, D. A., Danabasoglu, G., Jochum, M., Kiehl, J. T., Levis, S., and Park, S.: The Low-Resolution CCSM4, Journal of Climate, 25, 3993–4014, https://doi.org/10.1175/JCLI-D-11-00260.1, 2012.

Simstich, J., Sarnthein, M., and Erlenkeuser, H.: Paired δ^{18}O signals of *Neogloboquadrina pachyderma* (s) and *Turborotalita quinqueloba* show thermal stratification structure in Nordic Seas, Marine Micropaleontology, 48, 107–125, https://doi.org/10.1016/S0377-8398(02)00165-2, 2003.

Skinner, L. C. and Elderfield, H.: Constraining ecological and biological bias in planktonic foraminiferal Mg/Ca and δ^{18}O$_{cc}$: A multispecies approach to proxy calibration testing, Paleoceanography, 20, PA1015, https://doi.org/10.1029/2004PA001058, 2005.

Smith, R., Jones, P., Briegleb, B., Bryan, F., Danabasoglu, G., Dennis, J., Dukowicz, J., Eden, C., Fox-Kemper, B., Gent, P., Hecht, M., Jayne, S., Jochum, M., Large, W., Lindsay, K., Maltrud, M., Norton, N., Peacock, S., Vertenstein, M., and Yeager, S.: The Parallel Ocean Program (POP) reference manual: Ocean component of the Community Climate System Model (CCSM) and Community Earth System Model (CESM), Tech. rep., Los Alamos National Laboratory, 2010.

Spezzaferri, S., Kucera, M., Pearson, P. N., Wade, B. S., Rappo, S., Poole, C. R., Morard, R., and Stalder, C.: Fossil and Genetic Evidence for the Polyphyletic Nature of the Planktonic Foraminifera "*Globigerinoides*", and Description of the New Genus *Trilobatus*, PLoS ONE, 10, 1–20, https://doi.org/10.1371/journal.pone.0128108, 2015.

Stangeew, E.: Distribution and Isotopic Composition of Living Planktonic Foraminifera *N. pachyderma* (sinistral) and *T. quinqueloba* in the High Latitude North Atlantic, Ph.D. thesis, Christian-Albrechts-Universität zu Kiel, 2001.

Stewart, I. A., Darling, K. F., Kroon, D., Wade, C. M., and Troelstra, S. R.: Genotypic variability in subarctic Atlantic planktic foraminifera, Marine Micropaleontology, 43, 143–153, https://doi.org/10.1016/S0377-8398(01)00024-X, 2001.

Storz, D., Schulz, H., Waniek, J. J., Schulz-Bull, D. E., and Kučera, M.: Seasonal and interannual variability of the planktic foraminiferal flux in the vicinity of the Azores Current, Deep-Sea Research I, 56, 107–124, https://doi.org/10.1016/j.dsr.2008.08.009, 2009.

5   Taboada, F. G. and Anadón, R.: Seasonality of North Atlantic phytoplankton from space: Impact of environmental forcing on a changing phenology (1998-2012), Global Change Biology, 20, 698–712, https://doi.org/10.1111/gcb.12352, 2014.

Thiede, J.: Distribution of foraminifera in surface waters of a coastal upwelling area, Nature, 253, 712–714, https://doi.org/10.1038/253712a0, 1975.

Ting, C. S., Rocap, G., King, J., and Chisholm, S. W.: Cyanobacterial photosynthesis in the oceans: The origins and significance of divergent

10   light-harvesting strategies, Trends in Microbiology, 10, 134–142, https://doi.org/10.1016/S0966-842X(02)02319-3, 2002.

Watkins, J. M., Mix, A. C., and Wilson, J.: Living planktic foraminifera: tracers of circulation and productivity regimes in the central equatorial Pacific, Deep Sea Research II, 43, 1257–1282, 1996.

Watkins, J. M., Mix, A. C., and Wilson, J.: Living planktic foraminifera in the central tropical Pacific Ocean: Articulating the equatorial 'cold tongue' during La Niña, 1992, Marine Micropaleontology, 33, 157–174, https://doi.org/10.1016/S0377-8398(97)00036-4, 1998.

15   Wilke, I., Meggers, H., and Bickert, T.: Depth habitats and seasonal distributions of recent planktic foraminifers in the Canary Islands region (29ºN) based on oxygen isotopes, Deep-Sea Research I, 56, 89–106, https://doi.org/10.1016/j.dsr.2008.08.001, 2009.

Wolfteich, C. M.: Satellite-Derived Sea Surface Temperature, Mesoscale Variability, and Foraminiferal Production in the North Atlantic, M.Sc., Cambridge, MS, 1994.

Yu, E.-F., Francois, R., Bacon, M. P., Honjo, S., Fleer, A. P., Manganini, S. J., Rutgers van der Loeff, M. M., and Ittekot, V.: Trapping

20   efficiency of bottom-tethered sediment traps estimated from the intercepted fluxes of ^{230}Th and ^{230}Pa, Deep-Sea Research Part I, 48, 865–889, https://doi.org/10.1016/S0967-0637(00)00067-4, 2001.

Žarić, S., Donner, B., Fischer, G., Mulitza, S., and Wefer, G.: Sensitivity of planktic foraminifera to sea surface temperature and export production as derived from sediment trap data, Marine Micropaleontology, 55, 75–105, https://doi.org/10.1016/j.marmicro.2005.01.002, 2005.

25   Žarić, S., Schulz, M., and Mulitza, S.: Global prediction of planktic foraminiferal fluxes from hydrographic and productivity data, Biogeosciences, 3, 187–207, 2006.
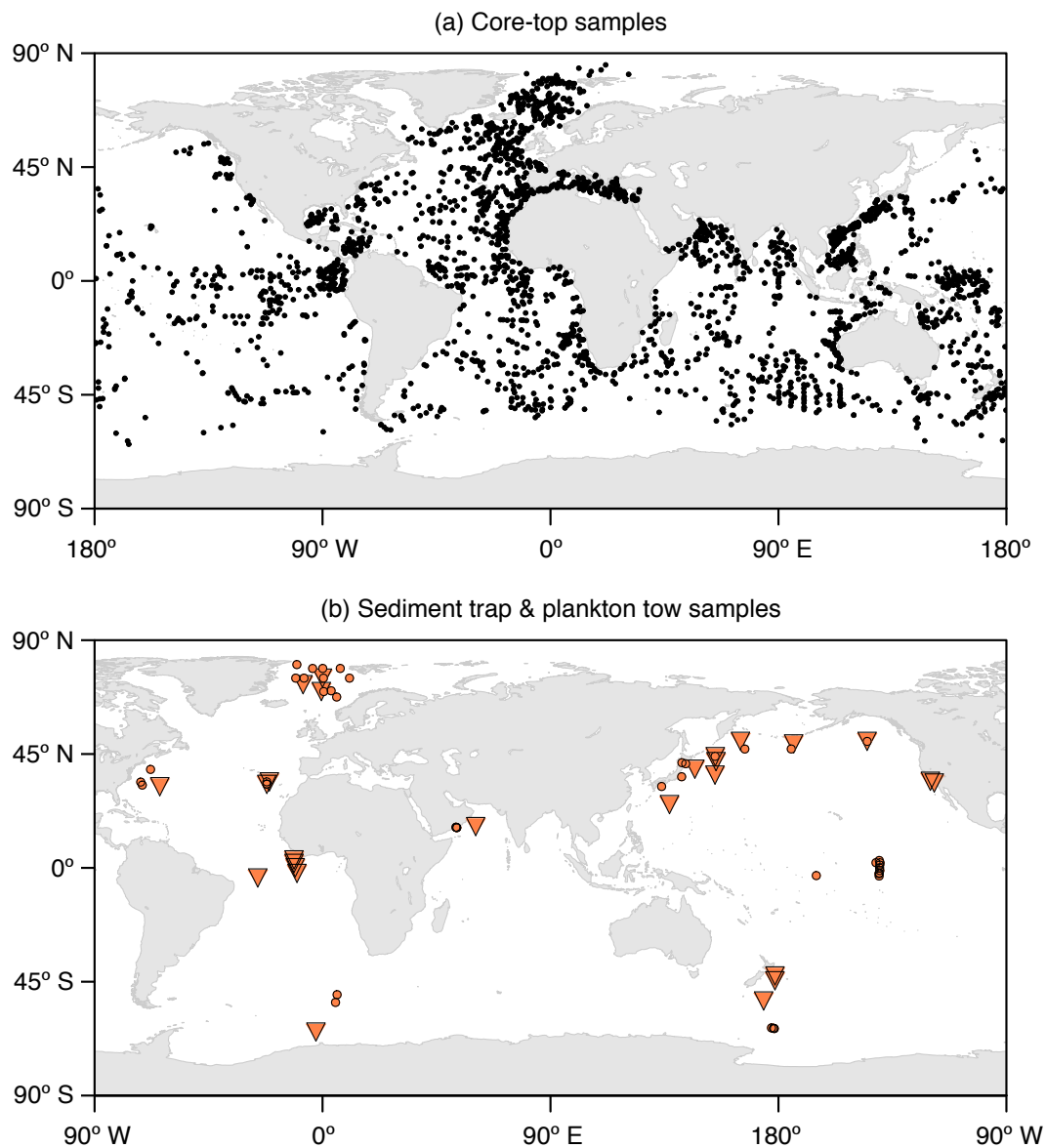
Figure 1. Locations of (a) the core-top samples with planktonic foraminifera counts and (b) the plankton tow (orange circles) and sediment trap (orange triangles) samples used for the model validation. The map in Figure 1a shows a combination of the data sets of Prell et al. (1999), Pflaumann et al. (1996, 2003), and Kucera et al. (2005). The respective information on the sediment trap and plankton tow data shown in Figure 1b is given in Tables S1 and S2 in the Supplement.
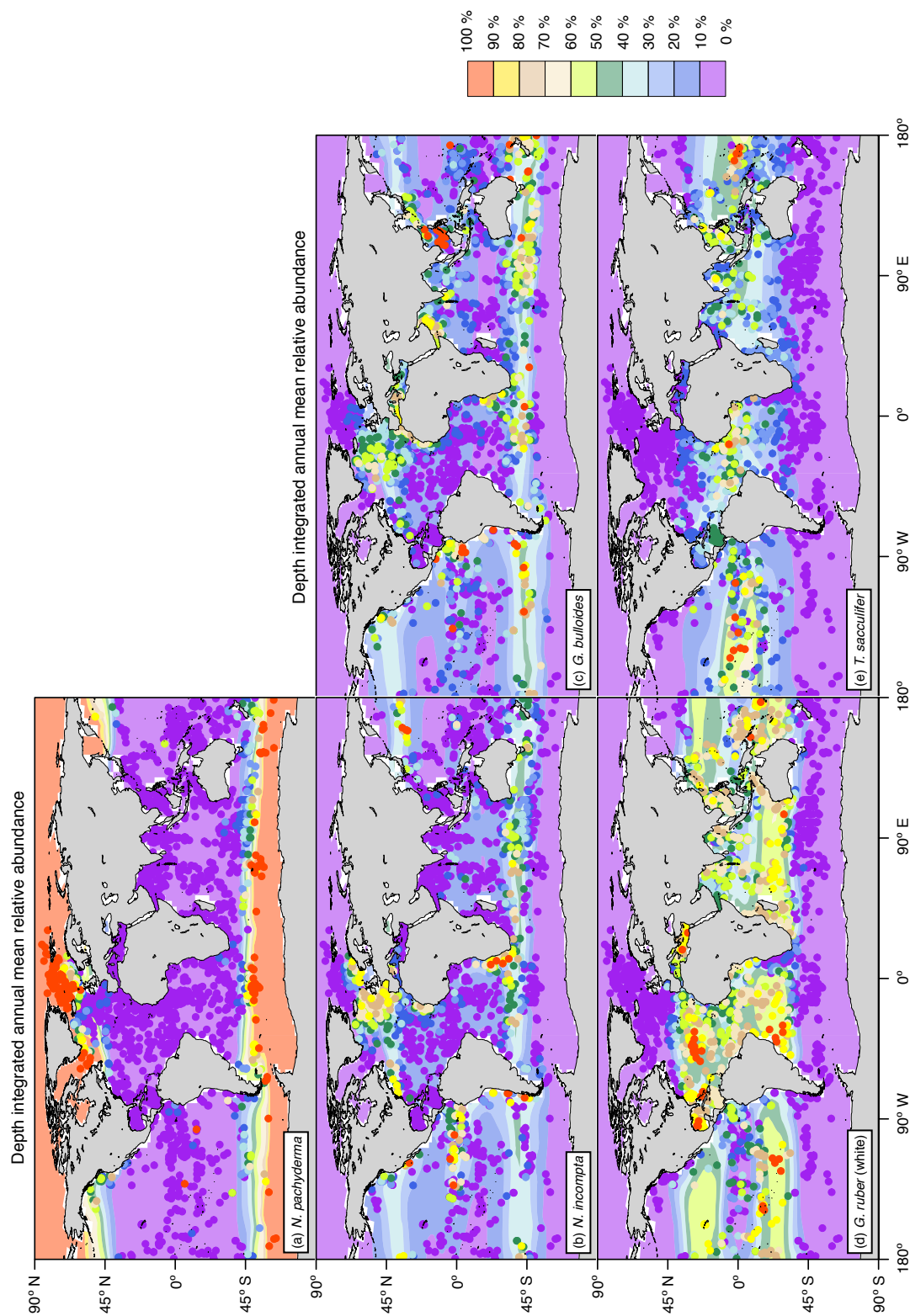
Figure 2. Relative abundances of the depth integrated modeled annual mean concentration (pale-colored contours; % biomass) and of the core-top samples (circles; % individuals) for (a) *N. pachyderma*, (b) *N. incompta*, (c) *G. bulloides*, (d) *G. ruber* (white), and (e) *T. sacculifer*. The relative abundances consider only the five foraminiferal species included in PLAFOM2.0. Note that we are aware that for a small number of core-top samples the relative abundances of the individual planktonic foraminiferal species are overestimated due to the recalculations by only considering *N. pachyderma*, *N. incompta*, *G. bulloides*, *G. ruber* (white), and *T. sacculifer* rather than the whole assemblage. However, the overall general pattern does not change and can, thus, be used for the model-data comparison.
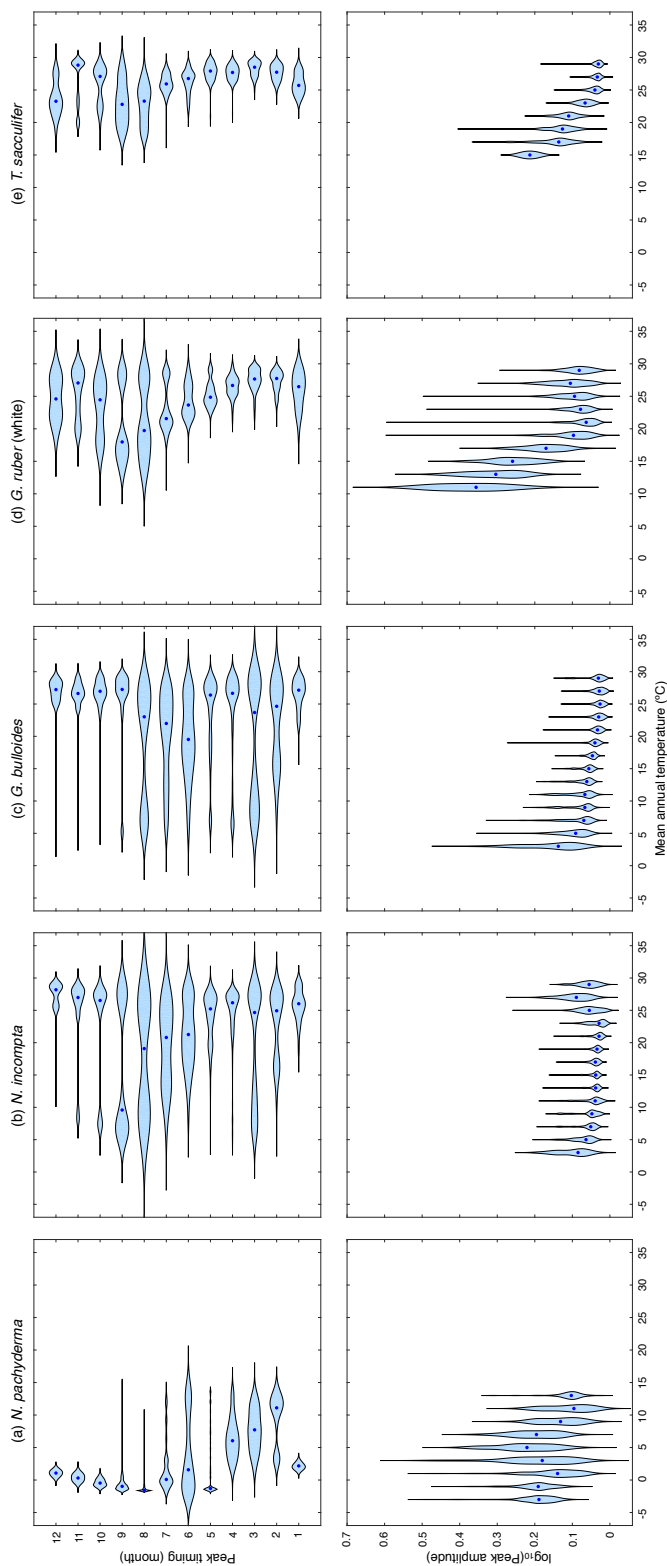
Figure 3. Violin plots showing the dependence of the modeled peak timing (top row) and/or the modeled peak amplitude (bottom row) on the annual mean temperature (in °C) averaged over the top 55 m of the water column for (a) *N. pachyderma*, (b) *N. incompta*, (c) *G. bulloides*, (d) *G. ruber* (white), and (e) *T. sacculifer*. The modeled peak timing is given in months and the modeled peak amplitude has been log-transformed. The blue dots represent the respective median values. Note that the peak timings of each species from the southern hemisphere have been transformed to northern hemisphere equivalents by adding or subtracting 6 months.
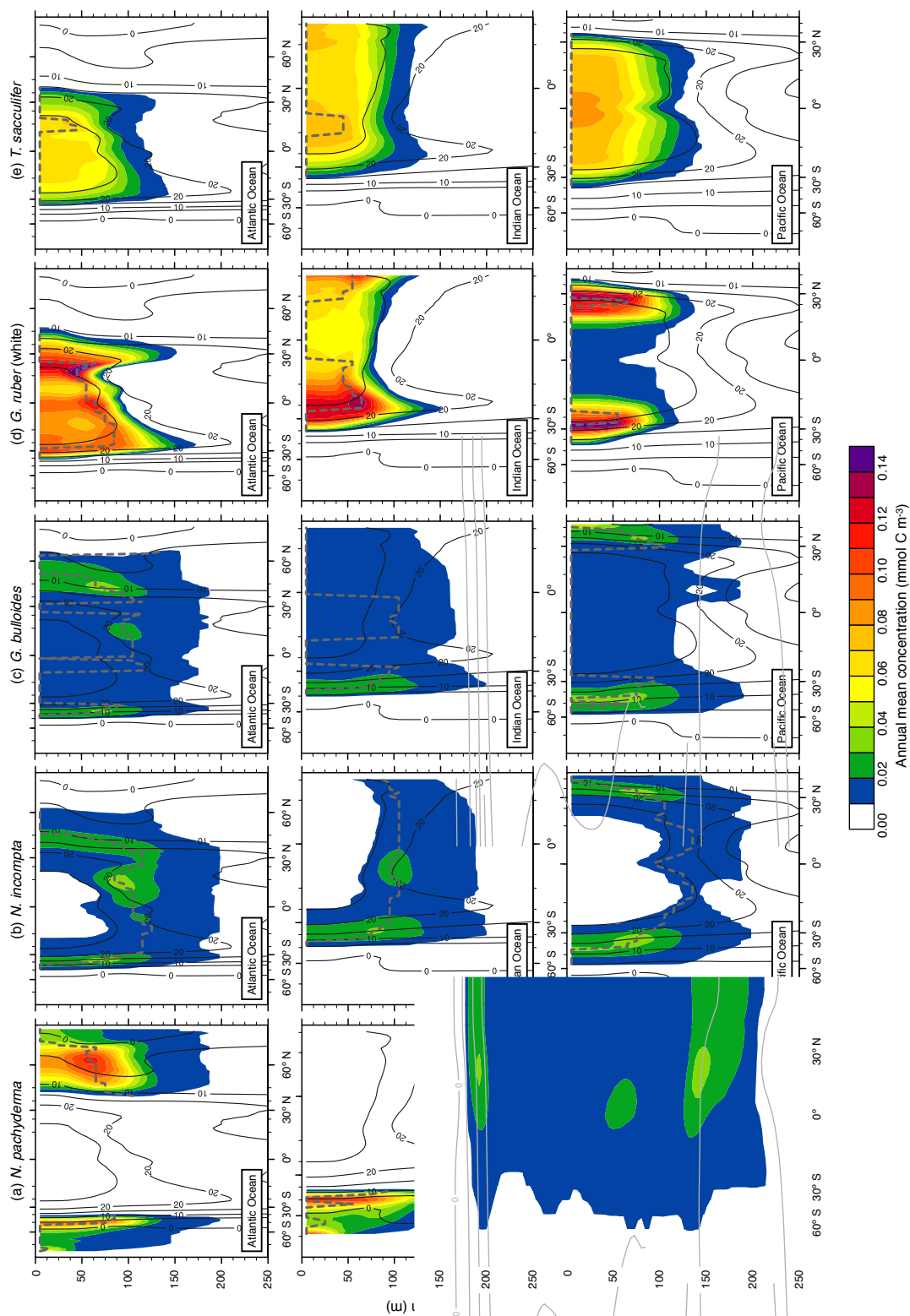
Figure 4. Depth transects of the modeled annual mean concentration (mmol C m^{-3}) along $\sim 27\,°$W in the Atlantic Ocean (top row), $\sim 71\,°$E in the Indian Ocean (middle row), and $\sim 162\,°$W in the Pacific Ocean (bottom row) over the top 250 m for (a) *N. pachyderma*, (b) *N. incompta*, (c) *G. bulloides*, (d) *G. ruber* (white), and (e) *T. sacculifer*. The dashed grey lines mark the depth of the maximum modeled annual mean production for each planktonic foraminiferal species respectively. The black contour lines indicate the annual mean temperature estimates. The blank areas denote where a species is absent.
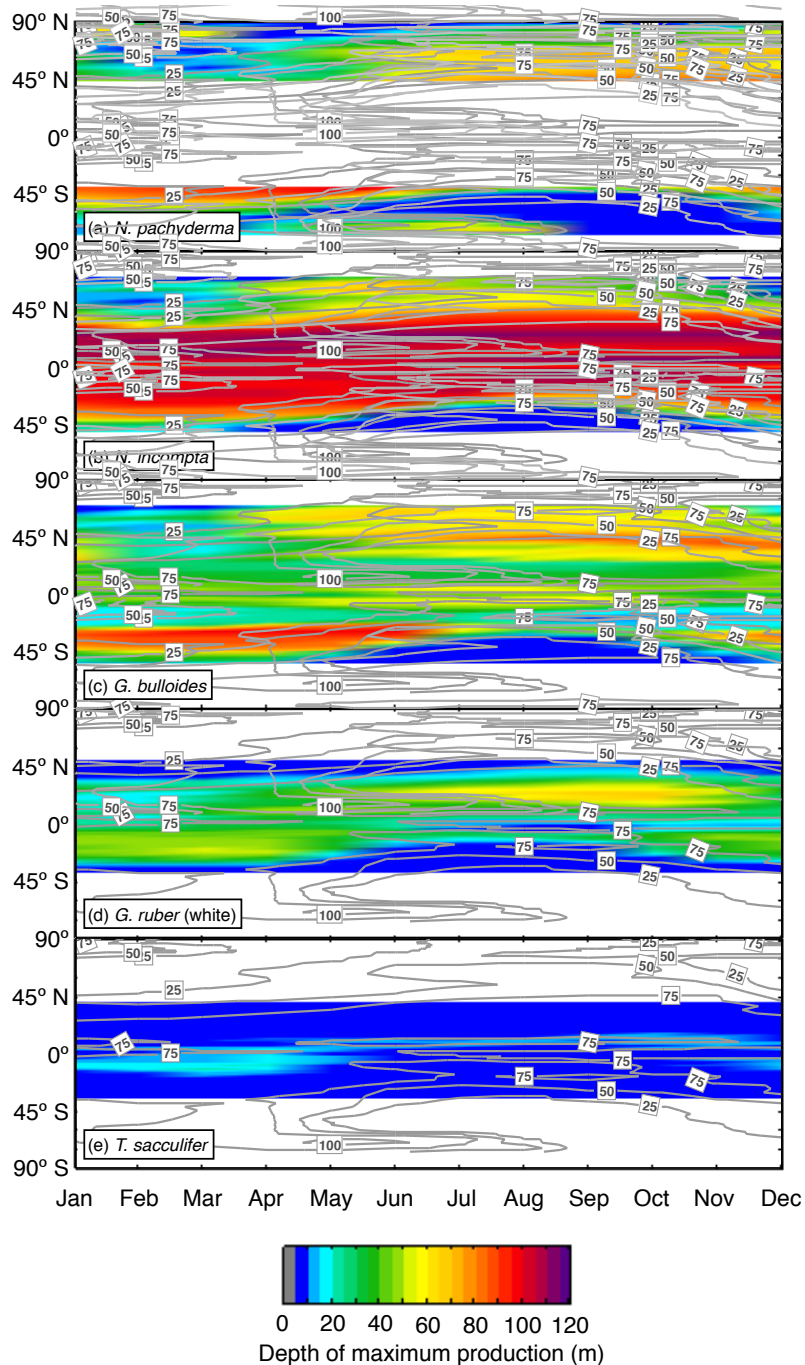
Figure 5. Zonal average of the depth (in m) at which the modeled maximum production of (a) *N. pachyderma*, (b) *N. incompta*, (c) *G. bulloides*, (d) *G. ruber* (white), and (e) *T. sacculifer* occurs over time. The grey contour lines indicate the zonal average of the (seasonally varying) depth of the chlorophyll maximum (in m). The blank areas denote where a species is absent.
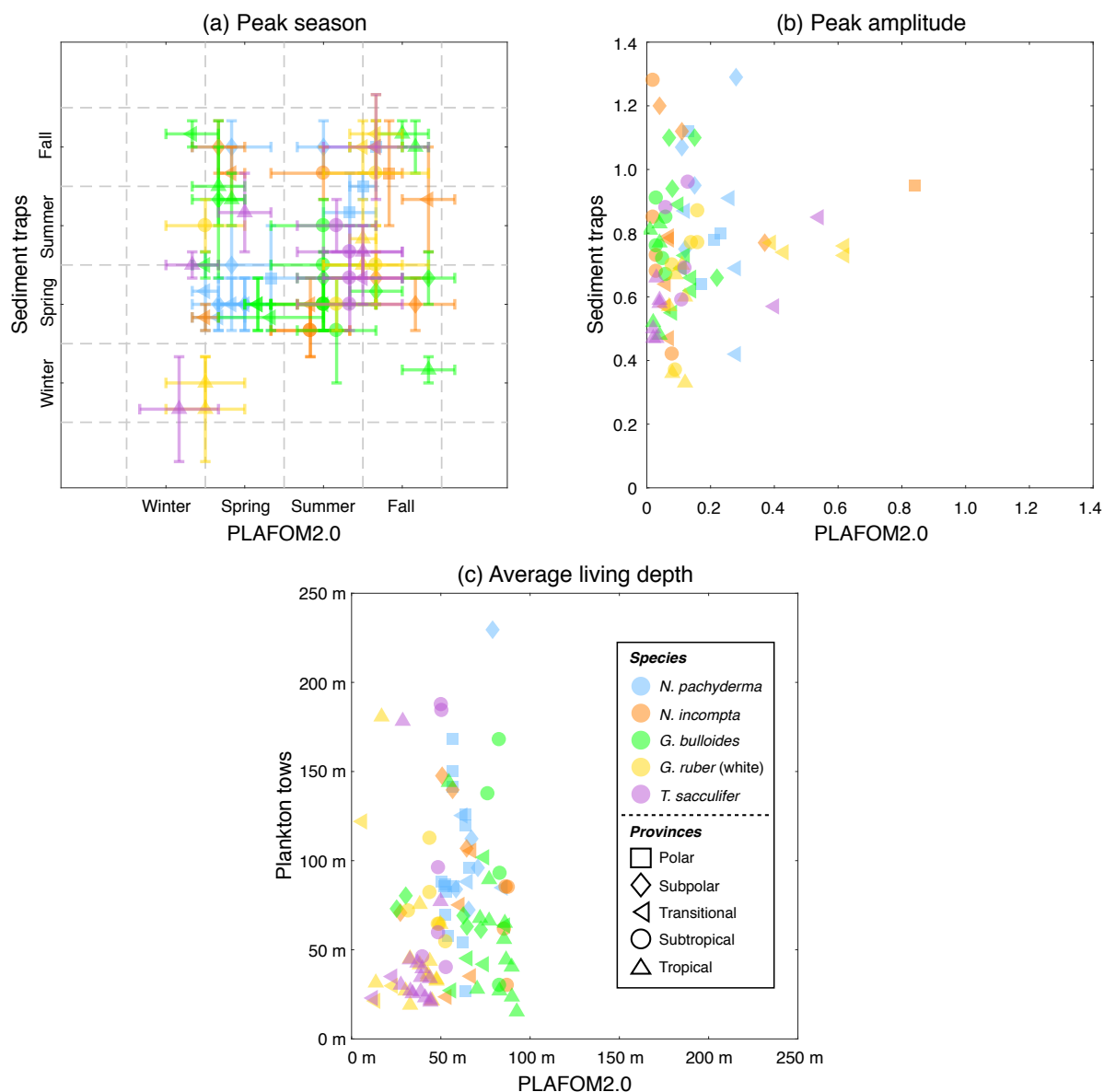
Figure 6. (a) Peak seasons (i.e., caloric season of the maximum production), (b) peak amplitudes (i.e., maximum production divided by annual mean), and (c) average living depths (in m) for *N. pachyderma* (light blue), *N. incompta* (orange), *G. bulloides* (green), *G. ruber* (white) (gold), and *T. sacculifer* (orchid) based on either the sediment trap data (given in Table S3) or the plankton tow data (given in Table S4) vs. PLAFOM2.0. The symbols represent the polar (squares), subpolar (diamonds), transitional (left-pointing triangles), subtropical (circles), and tropical (upward-pointing triangles) provinces of the ocean, respectively. The symbols in (a) indicate the month corresponding to the mid-season and the error bars refer to the overall time frame given in Table S3a.
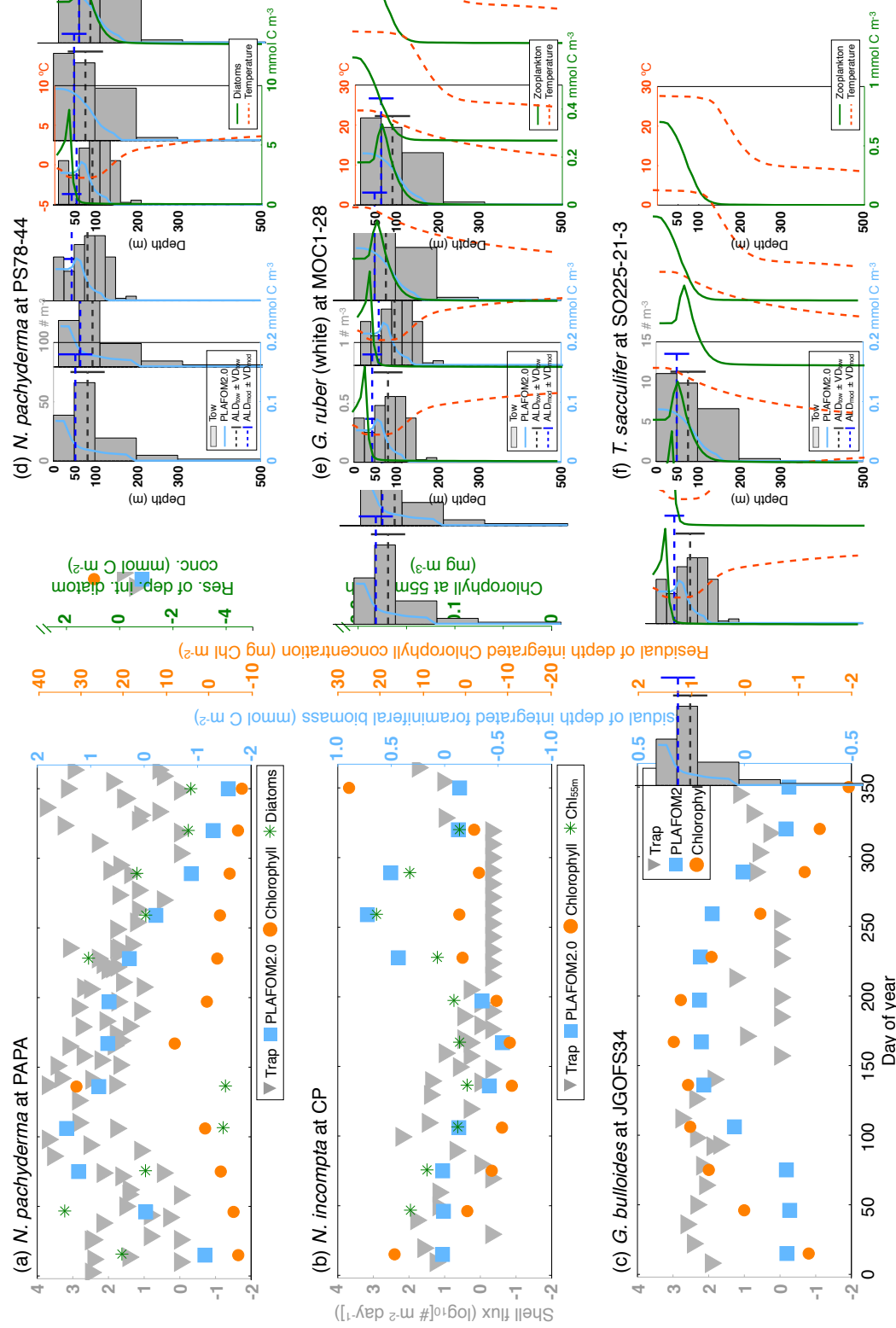
Figure 7. (a-c) Comparison of export planktonic foraminiferal shell fluxes in sediment traps (grey triangles) with the residuals (i.e., the deviation from the mean) of the depth integrated modeled foraminiferal biomass (light blue squares). Note that the difference in the units between sediment trap data ($\log_{10}[\#\,m^{-2}\,day^{-1}]$) and model output ($mmol\,C\,m^{-2}$) does not affect the assessment of peak timing. The orange circles denote the residuals of the depth integrated modeled chlorophyll concentration (in $mg\,Chl\,m^{-2}$), and the dark green asterisks indicate in (a) the residuals of the depth integrated modeled diatom concentration (in $mmol\,C\,m^{-2}$) and/or in (b) the chlorophyll concentration (in $mg\,m^{-3}$) at 55 m water depth. (d-f) Comparison of the vertical distribution of live specimens in plankton tows (in $\#\,m^{-3}$; grey bars) with the modeled foraminiferal concentration over depth (in $mmol\,C\,m^{-3}$; light blue profiles). The dashed dark grey and blue lines indicate the average living depth (in m) and vertical dispersion calculated for the plankton tows ($ALD_{tow} \pm VD_{tow}$) and PLAFOM2.0 ($ALD_{mod} \pm VD_{mod}$), respectively. The dashed red lines denote the predicted temperature profiles (in °C), whereas the dark green lines correspond to the modeled vertical distribution of (d) diatoms (in $mmol\,C\,m^{-3}$) and/or (e-f) zooplankton (in $mmol\,C\,m^{-3}$). Data series of (a) *N. pachyderma* at site PAPA, (b) *N. incompta* at site CP, and (c) *G. bulloides* at site JGOFS34. Depth profiles of (d) *N. pachyderma* at station PS78-44, (e) *G. ruber* (white) at station MOC1-28, and (f) *T. sacculifer* at station SO225-21-3. The respective locations of each sediment trap and plankton tow sample are given in Tables S1 and S2, respectively.

Table 1. Model parameter and their modifications relative to Fraile et al. (2008) and/or Kretschmer et al. (2016). The original value is given in parentheses.

Species	*N. pachyderma*	*N. incompta*	*G. bulloides*	*G. ruber* (white)	*T. sacculifer*
$P_{F,0}$	- (-)	- (-)	2.6 (-)	2.6 (-)	2.6 (-)
α_{PI}	- (-)	- (-)	0.012 (-)	0.01 (-)	0.07 (-)
$p_\%$	- (-)	- (-)	0.3 (-)	0.3 (-)	0.4 (-)
T_{thres}	18.0 (24.0)	3.0 (-0.3)	3.0 (-0.3)	10.0 (5.0)	15.0 (15.0)
$cl_{N.pachyderma,j}$	- (-)	0.2 (0.2)	0 (0)	0 (0)	0 (0)
$cl_{N.incompta,j}$	- (-)	- (-)	0.1 (0.1)	0.2 (0.8)	0 (0)
$cl_{G.bulloides,j}$	- (-)	0.8 (0.5)	- (-)	0.8 (0.8)	0.8 (0.8)
$cl_{G.ruber(white),j}$	- (-)	0.2 (0.8)	0.1 (0.5)	- (-)	0.2 (0.2)
$cl_{T.sacculifer,j}$	- (-)	0 (0)	0.1 (0.5)	0.2 (0.2)	- (-)

$P_{F,0}$ – maximum foraminiferal growth rate (day^{-1}) at $30\,^\circ$C (derived from the maximum zooplankton growth rate at $20\,^\circ$C given by Doney et al. (1996)).

α_{PI} – initial slope of the photosynthesis-light (PI) curve ($\mathrm{m}^2\,\mathrm{W}^{-1}\mathrm{day}^{-1}$) (derived from PI-curve of *Synechococcus* given in Jodłowska and Śliwińska (2014) for *G. bulloides* and of endosymbiotic dinoflagellates given in Jørgensen et al. (1985) for *T. sacculifer*).

$p_\%$ – fraction of photosynthesis contributing to foraminiferal growth rate.

T_{thres} – minimum (for *N. pachyderma*) or maximum (for all other species) threshold temperature at which foraminiferal species can thrive ($^\circ$C).

cl_{ij} – competition pressure of species i upon species j.